ACS OMEGA

Open Access

http://pubs.acs.org/journal/acsodf

Review

Label-Free and Rapid Microfluidic Design Rules for Circulating Tumor Cell Enrichment and Isolation: A Review and Simulation Analysis

Muhammad Asraf Mansor, Chun Yang, Kar Lok Chong, Muhammad Asyraf Jamrus, Kewei Liu, Miao Yu, Mohd Ridzuan Ahmad,* and Xiang Ren*

Cite This: *ACS Omega* 2025, 10, 6306−6322

Read Online

ACCESS | Metrics & More | Article Recommendations | Supporting Information

ABSTRACT: Enriching and isolating circulating tumor cells (CTCs) have attracted significant interest due to their important role in early cancer diagnosis and prognosis, allowing for minimally invasive approaches and providing vital information about metastasis at the cellular level. This review comprehensively summarizes the recent developments in microfluidic devices for CTC enrichment and isolation. The advantages and limitations of several microfluidic devices are discussed, and the design specifications of microfluidic devices for CTC enrichment are highlighted. We also developed a set of methodologies and design rules of label-free microfluidics such as spiral, deterministic lateral displacement (DLD) and dielectrophoresis (DEP) to allow researchers to design and develop microfluidic devices systematically and effectively, promoting rapid research on design, fabrication, and experimentation.

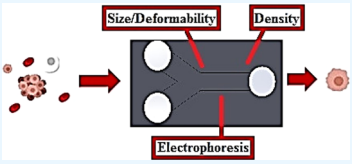

INTRODUCTION

Cancer metastasis is a complex series of steps in which cancer cells migrate from the original tumor location to nearby organs. This process begins with the emergence of the primary tumor, where cancer cells progressively grow and infect the nearby stroma and tissues, including the blood and lymphatic arteries.[1,2] At this stage, the intravasated tumor cells grow adaptively to enhance their survival rate in the challenging environment of the bloodstream. These cells are known as "circulating tumor cells" (CTCs), and they are an essential part of cancer metastasis.[3,4] Their quantity, appearance, and genetic properties provide extensive multivariate insights into primary tumor. CTCs were first reported in 1969 by Ashworth, who discovered the presence of cells in the blood of a metastatic cancer patient. These cells resembled the morphological features of cancer cells found in the original tumors.[5,6] CTCs are tumor cells that detach from the primary tumor and subsequently enter the bloodstream to circulate. CTCs have the ability to circulate in the bloodstream either as individual cells or as clusters. Both forms of CTCs have the capacity to metastasize and invade surrounding tissues.[7] The CTCs occur rarely, and in general, in the bloodstream, a single CTC is surrounded by approximately 1 million white blood cells (WBCs) and 1 billion red blood cells (RBCs) per milliliter.[8] Therefore, achieving an excellent level of efficiency and selectivity in capturing CTCs is the initial and critical step in a CTC-based analysis. A CTC cluster is a group or cluster of two or more CTCs that are found traveling together in the bloodstream, often physically attached to each other.[9] The clustering of CTCs has been demonstrated as an adaptive strategy that improves the survival of CTCs in aggressive blood circulation and facilitates their ability to spread to other parts of the body.[10,11] Compared with individuals, a CTC cluster has a much higher rate of metastasis, ranging from 20 to 100 times higher, in several cancer types including breast and prostate cancer. Moreover, these clusters are linked to a more unfavorable prognosis and reduced overall survival rates among cancer patients.[12] CTC clusters may consist of multiple tumor cells in different states, leading to complicated metastasis properties. Thus, it is important to analyze the molecular and genetic properties of individual CTCs to avoid information loss and misunderstandings.[13−15] Hence, comprehending the unique and captivating characteristics of a single CTC is a crucial element in the advancement of biomedical research for CTC analysis. Major researchers have developed technologies to enhance the separation and detection of CTCs. The density gradient centrifugation method was the initial method used to eliminate RBCs or plasma to enrich and collect CTCs, on the top layer of the blood sample.[16] Devices such as OncoQuick assay (Greiner BioOne) and Ficoll are commercially available.[17,18] The density gradient centrifugation method is considered cost-effective and simple to use; however, this method has drawbacks such as high loss of CTCs and poor enrichment results.[19] This classical method could also lead to unwanted activation of sensitive immune cells[20] and platelets to interfere with the analysis of CTCs.[21]

Received: September 19, 2024
Revised: January 25, 2025
Accepted: January 29, 2025
Published: February 11, 2025

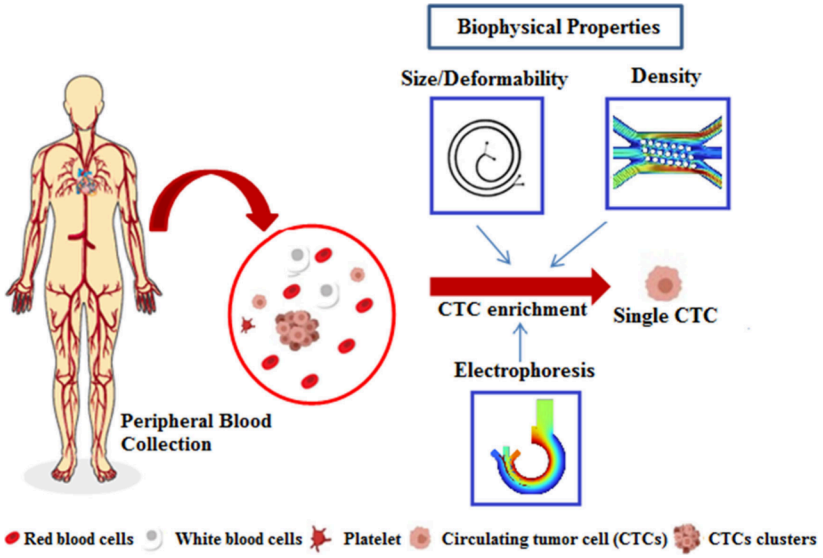

Figure 1. Schematic diagram of various techniques for enrichment and isolation of CTCs based on their biophysical characteristic differences.

Table 1. Summary of Size-Based Microfluidic Techniques for CTC Enrichment

Technology	Mechanism	Flow rate	Capture efficiency	Capture purity	Enrichment label	Microfilter shape	Cell line
PMM[36]	Filtration	10 mL/h	>90.0%	NA	Label-free	Circular 9.1 μm diameter	A549, SK-MES-1, and H446 cells
FAST[45]	Filtration	>3 mL/min	95.9 ± 3.1%	>2.5 log depletion of WBCs	Label-free	Circular 8 μm diameter	MCF-7, MDA-MB-231, and MDA-MB-436, HCC78, and AGS cells
Channel[46]	Filtration	~0.4 mL/h	>92.0%	NA	Label-free	Filtration channel 5 μm height	A459, SK-MES-1 and H446 cells
MCA1[40]	Filtration	200−1000 μL/min	~80.0%	NA	Label-free	Circular 8.4−9.1 μm diameter	NCI-H358 cells
MCA2[39]	Filtration	200 μL/min	~80.0%	Improved purity than MCA1	Labe-free	Rectangular 5−9 μm width and 30 μm length	NCI-H358 cells
3D-printed[47]	Hybrid	2 mL/h	>90.0%	~2.34 log depletion of WBCs	CD45 antibody	Circular 3 μm diameter	MDA-MB-231 cells
SB microfilters[48]	Filtration	gravity	78.0−83.0%	NA	Label-free	Circular top-40 μm Circular bottom-8 μm Gap distance-10 μm	MCF-7 and MDA-MB-231 cells
CROSS[49]	Filtration	80 μL/min	~70.0%	7.2%	Label-free	Micropillars 25 μm spaced 5 μm	SW480 cells
ETFE filter[44]	Filtration	1 mL/min	~96.0%	NA	Label-free	Circular 7 μm diameter	NCI-H358 cells
Integrated microfluidic[50]	Filtration	0.2 mL/min	>73.0%	NA	Label-free	Pore microchannel 8 μm	Caco-2 cells
Size and Invasiveness[51]	Filtration	FBS gradient	74.0 ± 14.0% to 88.2 ± 9.1%	83.93 ± 0.63%	Label-free	Gap 8 μm	HEK-293, CL-187, MGC-803, and SGC-7901 cells
Integrated Microfluidic[52]	Hybrid	gravity	85.0%	NA	CD45	Circular 10 μm	PC-9 cells
RCT[53]	Filtration	600 μL/h	>90.0%	NA	Label-free	Trapping channel minimum size of 5 μm	UM-UC13 cells
Fluid-assisted Separation[54]	Hybrid	NA	95.8%	99.72% depletion of WBCs	Label-free	Pore diameter of 6.881 ± 0.592 μm	HeLa, SW620, and MDA-MB-231 cells
Pressure-Sensing Microfiltration[55]	Filtration	1 mL/min	>96.0%	>99% depletion of WBCs	Label-free	Circular 7 μm diameter	H358 cells
The Cluster-Chip[56]	Filtration	2.5 mL/h	100%	NA	Label-free	3 triangular pillars with the 12 μm openings	MDA-MB-231, MCF-7, LBX1 cells
Automated microfiltration[57]	Filtration	2 mL/min	>93.0%	1.64 ± 0.22%	Label-free	Square-shaped pores of 7, 8, and 9 μm	PC-3 cells
Windmill-like hole array[58]	Filtration	2 mL/min	93% for A549 cells; 90% for HeLa	98.7% depletion of WBCs	Label-free	7 × 35 μm windmill-like hole array	A549 and HeLa cells

Microfluidics has significantly promoted biomedical research by allowing for the manipulation of tiny blood volumes and precisely controlling the cellular microenvironment, resulting in remarkable sensitivity and efficiency. Currently, there are two primary approaches for CTC enrichment using microfluidic techniques: affinity-based methods and label-free methods.[22] The affinity-based microfluidic technique involves capturing CTCs based on their surface protein expression

https://doi.org/10.1021/acsomega.4c08606
ACS Omega 2025, 10, 6306−6322

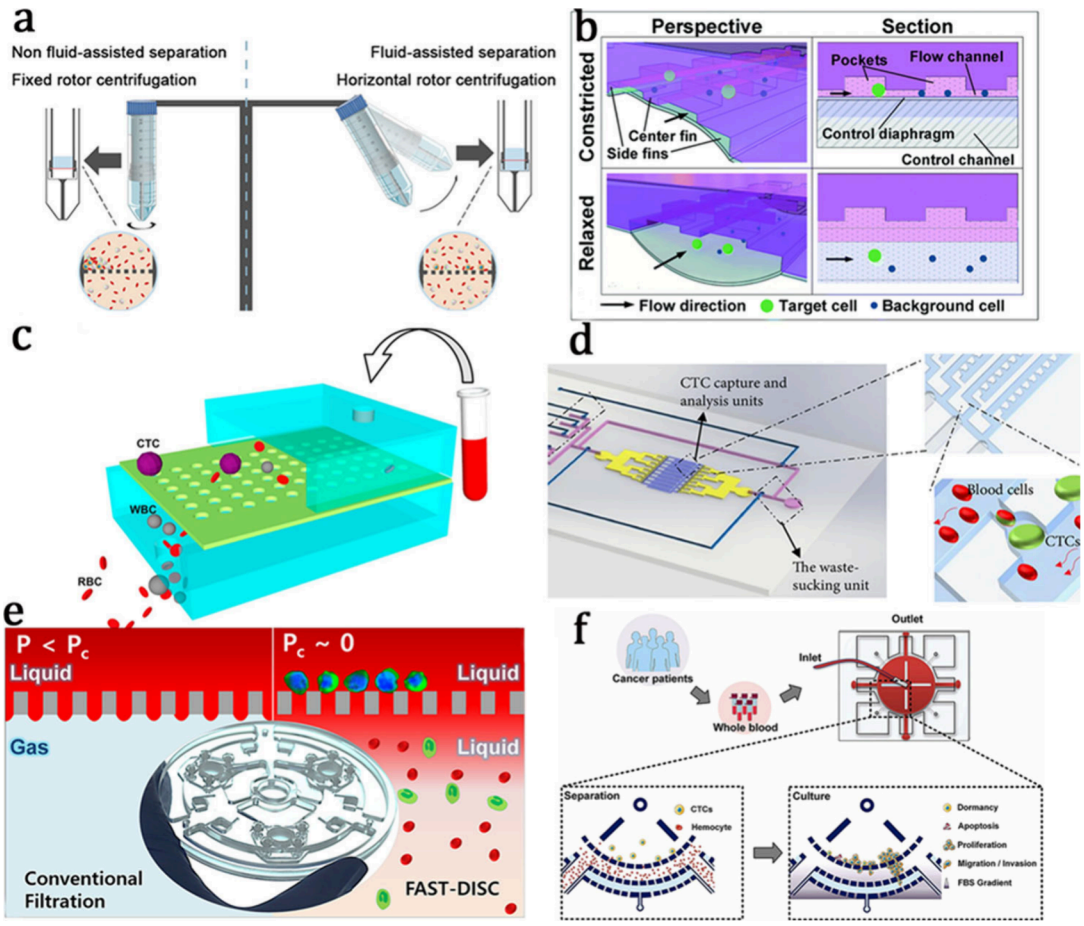

Figure 2. Microscopy images of various membrane microfilters for CTC enrichment. (a) Schematic illustration of the centrifugal process and the performance of blood cells on the membrane during centrifugation. Reprinted with permission from ref 54. Copyright 2022, American Chemical Society. (b) Schematic illustration of the device function in different states. Reprinted with permission from ref 53. Copyright 2015, Royal Society of Chemistry. (c) Schematic of the microfluidic device integrated with PMM. Reprinted with permission from ref 36. Copyright 2015, Elsevier. (d) A schematic representing how larger cancer cells got trapped in the chamber, while small blood cells escaped. Reprinted with permission from ref 50. Copyright 2023, John Wiley & Sons. (e) Schematic illustration shows the mechanism of the fluid-assisted separation technology disc. Reprinted with permission from ref 45. Copyright 2017, American Chemical Society. (f) Enrichment principle of the system for functional CTCs. Reprinted with permission from ref 51. Copyright 2023, Elsevier.

levels, including particular antibodies or aptamers, and allows for the identification of cancer-specific biomarkers. The EpCAM is one of the current gold standards used in affinity-based methods. However, a population of CTCs is heterogeneous and may experience the epithelial-mesenchymal transition (EMT) phenomenon to interfere with the analysis of CTCs.[23,24]

Meanwhile, the label-free methods utilizing intrinsic physical cell characteristics for cell separation and isolation (without relying on antibodies) are highly cost-effective, fast diagnostics, with enhanced cell viability.[25−27] Nowadays, several methods are developed to enrich and isolate cells using microfluidic devices based on the biophysical properties of CTCs, such as size, deformability, density, and electrical polarizability, compared with leukocytes (Figure 1). These approaches may overcome the potential bias toward epithelial antigens that is inherent in immunocapture methods in label-based methods.[28] In addition, the label-free approaches are compatible with a larger range of assessments to maintain CTCs' physical integrity. Several recent reviews on CTC enrichment have only focused on current technology development to isolate and detect CTCs.[29−34] This review comprehensively summarizes the recent development in microfluidic devices for CTC enrichment and isolation. To provide a systematic and effective approach to designing and developing microfluidic devices, we also highlight the design rule specification of several microfluidic CTC enrichment techniques. The label-free approach is independent of the expression of specific biomarkers of the CTCs. Tumor cells penetrating into the bloodstream may lead to metabolic abnormalities, gene expression, and cell composition change. As a result, the altered biophysical properties of CTCs, such as density, size, deformability, and electric charge, can be utilized to separate and isolate CTCs from other blood cells.

SIZE AND DEFORMABILITY-BASED ENRICHMENT

Various techniques, such as centrifugation, magnetic separation, microchips, filtration, micro/nano substrates, and biomarkers, have been applied to detect and enrich CTCs. Microfluidic devices for CTC enrichment provide cost-effective and simply automated operation, offering precise control over the flow behaviors of CTCs within microchannels. The utilization of microfluidic techniques has enhanced the efficiency and reliability of CTC enrichment technologies from

https://doi.org/10.1021/acsomega.4c08606
ACS Omega 2025, 10, 6306−6322

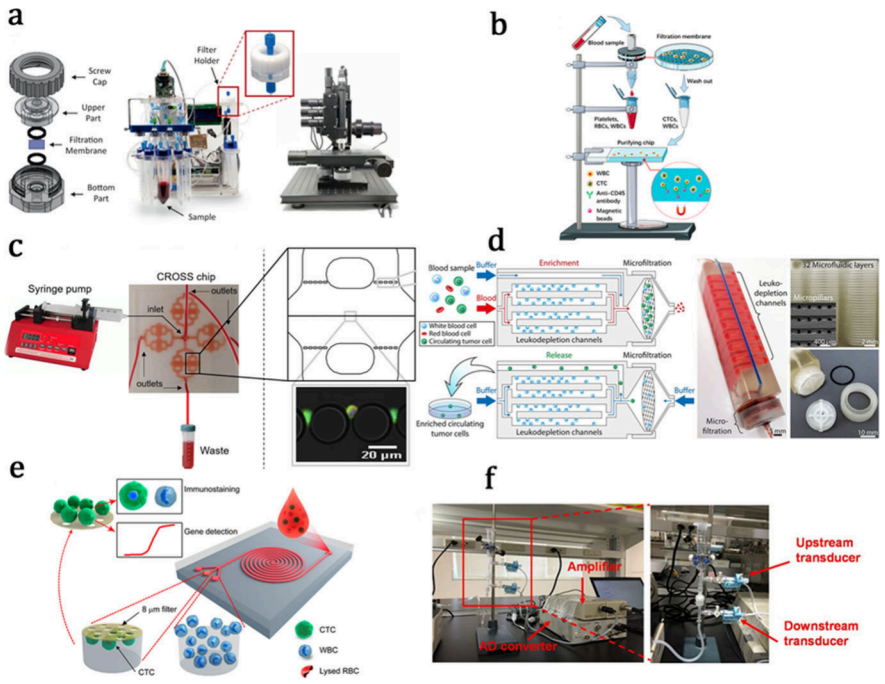

Figure 3. CTC enrichment device setup. (a) Schematic showing the parts that compose the holder where the membrane is placed. A blood sample is automatically processed through the microfiltration device, followed by immunostaining steps. The membrane is mounted on a microscope slide, and images are acquired using the integrated imaging system. Reprinted with permission from ref 57. Copyright 2020, Springer Nature. (b) Schematic illustration of the integrated microfluidic CTC isolation platform. Reprinted with permission from ref 52. Copyright 2021, MDPI. (c) Experimental setup for CTC isolation using the CROSS chip. Reprinted with permission from ref 49. Copyright 2019, Springer Nature. (d) The design and operation principle of the 3D-printed microfluidic device. Reprinted with permission from ref 47. Copyright 2021, Springer Nature. (e) Schematic illustrations of the circulating tumor cell enrichment process using the developed device. Reprinted with permission from ref 63. Copyright 2015, American Chemical Society. (f) Measurement of differential pressure in microfiltration and photograph of the pressure sensing module. Reprinted with permission from ref 55. Photograph courtesy of Daisuke Onoshima; copyright 2022, American Chemical Society.

label-based to size-based microfluidic devices.[35] CTCs exhibit distinct morphological features, such as variations in size, deformability, and cellular electrical properties.[36] Label-free methods have been recognized as viable alternatives to immune-based techniques.

The principle of size-based CTC enrichment relies on the geometric properties and deformability of CTC. Size-based enrichment methods can be categorized into two types: microfilters and microfluidic CTC sorting devices.[37] Table 1 shows a summary of size-based microfluidic techniques for CTC enrichment. This review captures efficiency and purity to assess the performance of a CTC enrichment technique using tumor cell spiked whole blood samples. The number of spiked tumor cells enables the counting of both isolated tumor cells and leukocytes to determine both the efficiency and purity. Despite achieving approximately a 4-log reduction of leukocytes, the remaining nonspecific leukocytes still range from 10^3 to 10^4.[38] Counting the exact number of residual leukocytes becomes challenging, especially when only a few spiked tumor cells are present in the cell mixture. To apply this approach to clinical patients, a higher detection sensitivity is required. To objectively assess a technique's performance, CellSearch, an FDA-approved CTC diagnostic platform, is utilized to compare the number of detected CTCs in 7.5 mL of blood and the count of patients with positive CTCs.

Numerous microfluidic platforms have been reported for enriching CTCs based on cell size and deformability. Membrane filters are used to separate CTCs from whole blood samples based on the size differences between cancer cells and leukocytes.[36] With advancements in microfabrication techniques, filters with varying types and densities of pores can be precisely manufactured for CTC enrichment. Most reported filters with pore sizes around 6−10 μm in diameter demonstrated effectiveness.[38−40] Microfilters utilizing lithography show uniformly distributed pores for the effective and efficient enrichment of CTCs. It is considered a high throughput and label-free process due to the rapid processing of large amounts of samples through membrane filter platforms.[41] Microfiltration often encounters issues such as clogging, high-pressure drops, and compromised cell viability.[39,42] In response to these challenges, optimization strategies are used to adjust parameters such as dimensions, geometric configurations, and material properties. Fan et al. designed and developed a polydimethylsiloxane (PDMS) membrane filter-based technique for the enrichment of CTCs.[36] They used an economical sandwich molding technique along with a layer-based thin-film transferring method to create microfilters with PDMS (Figure 2c). This approach has only one photolithography step and one deep reactive ion etching step for the molding master fabrication. They utilized a water-soluble poly(vinyl alcohol) (PVA) film as a transfer support layer to address the softness of thin PDMS during transferring.[43] With the same emphasis on membrane material, N. Kihara has reported the development of an optically transparent ethylene tetrafluoroethylene (ETFE) membrane filter, characterized by several tens of millions of bored through-holes.[44] This filter is designed for the filtration of CTCs in the whole blood and features 380000 straight and precisely aligned holes (diameter 7 μm), covering an area of 13 mm in diameter. In a separation test, CTC model cells spiked into the whole blood using this

https://doi.org/10.1021/acsomega.4c08606
ACS Omega 2025, 10, 6306−6322

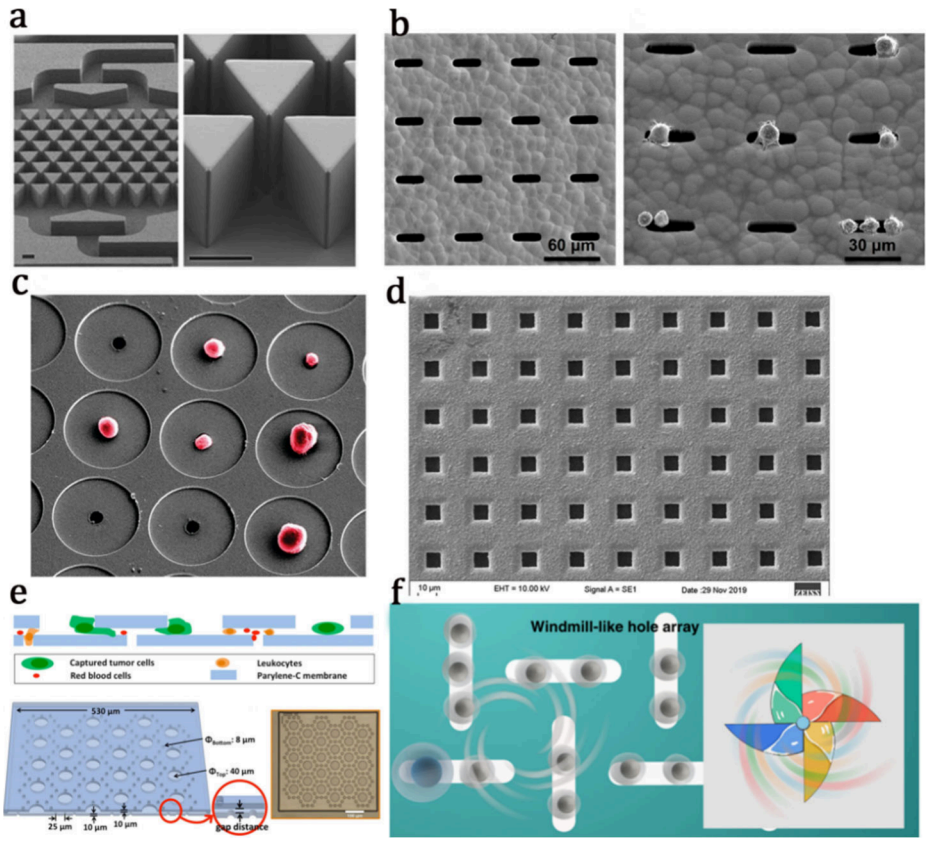

Figure 4. Geometry difference of microfilters. (a) SEM micrographs of the cluster chip showing multiple rows of shifted triangular pillars that form consecutive cluster traps (left) and a high-magnification image of a cluster trap (right). Scale bars: 60 μm. Reprinted with permission from ref 60. Copyright 2018, Elsevier. (b) SEM image of the rectangular MCA. SEM image of NCI-H69 cells trapped on a rectangular microcavity array (MCA). Reprinted with permission from ref 39. Copyright 2013, American Chemical Society. (c) Scanning electron microscope image of MCF-7 cells trapped on the microcavity array. The microcavities are 9 μm in size, with a 60 μm pitch. Reprinted with permission from ref 40. Copyright 2010, American Chemical Society. (d) SEM micrographs of a 7 μm pore size membrane, taken at 500× magnification. Reprinted with permission from ref 57. Copyright 2020, Springer Nature. (e) A cartoon of the device's cross-sectional view showing tumor cells captured along the edges of the large top Parylene-C pores. 3D view of an elemental unit model with key geometrical parameters labeled, including the gap distance in the inset. Reprinted with permission from ref 59. Copyright 2014, Springer Nature. (F) Schematic of the cell distribution on windmill-like membrane pores. Reprinted with permission from ref 58. Copyright 2022, Springer Nature.

fabricated microfiltration system demonstrate a high trapping efficiency of over 96%. Different membrane materials yield distinct filtration performances, which impacted subsequent observations during fluorescence staining.

The geometric configuration of the membrane pores was investigated by numerous research groups. Hosokawa has developed a microcavity array system for enriching CTC, featuring a circular pore design.[40] The device comprises a size-selective microcavity array to precisely segregate tumor cells from other blood cells, relying on their distinctions in both size and deformability. The device exhibits a relatively low capture purity and is susceptible to clogging. Besides modifying pore size, the conventional circular shape can be transformed into a rectangular array that enhances filtration efficiency and throughput.[39,40,57,58] To optimize this device, a new microcavity array system with a rectangular configuration for better capture results was developed for the shape and porosity of a microcavity array (MCA)[39] (Figure 4b), ensuring the efficient capture of small tumor cells on the microcavities with minimal flow resistance. Following the enhancement, the device achieved a capture efficiency exceeding 80%, with the flow rate remaining unaltered, and a notable enhancement in the depletion efficiency of white blood cells (Figure 4c).[40] Similarly, Yee-de León has developed an innovative membrane-based microfiltration device that includes a fully automated sample processing unit and a machine-vision-enabled imaging system.[57] The device incorporates square-shaped membranes characterized by pore diameters of 7, 8, and 9 μm, corresponding to porosities of 8.50%, 10.24%, and 11.98%, respectively (Figure 4d). In order to prevent any potential leakage during sample processing, each membrane is securely affixed within a custom-made PMMA holder comprising both upper and lower components, in addition to a screw cap (refer to Figure 3a).[57] Postfiltration, the imaging system's algorithm automatically identifies CTCs, and the accuracy is further verified by a trained operator.[38] Analysis of samples that were derived from healthy donors and spiked with various prostate cancer cell lines resulted in a capture efficiency of over 93%, ensuring the isolated cells' viability and suitability for subsequent molecular analysis. The microdevice developed by Li features an integrated design of the SU-8 membrane with a windmill-like hole array, inspired by the airflow disturbance phenomenon to enhance the enrichment of CTCs.[58] This windmill-like design introduces turbulence fluid, promoting cell self-mixing and pressure dispersion, resulting in increased fluid velocity (Figure 4f). Additionally, a lipid coating is applied to the membrane surface to prevent cell aggregation and hole clogging. Under optimal conditions, the platform

https://doi.org/10.1021/acsomega.4c08606
ACS Omega 2025, 10, 6306−6322

demonstrated notable recovery rates in a simulation with a CTC concentration of 20−100 cells per milliliter of blood. The recovery rates were 93% for A549 cells and 90% for HeLa cells. The platform exhibited a high white blood cell (WBC) depletion rate of 98.7%. Zhou introduced a separable bilayer microfilter for the enrichment of viable, size-based CTCs.[59] This device, unlike other single-layer CTC microfilters, features a precise gap between the two layers and a pore alignment architecture (Figure 4e). These characteristics significantly reduce the mechanical stress of CTCs, enabling their viable capture. The separation bilayer microfilter was tested with multiple cancer cell lines spiked into the blood of a healthy donor, demonstrating 78−83% high capture efficiency and 71−74% high retention of cell viability (Table 1). Sarioglu developed a microchip technology known as the Cluster-Chip to automatically capture clusters directly from unprocessed blood, to avoid using tumor-specific markers.[56] Specialized bifurcating traps are designed to operate under low-shear-stress conditions to preserve cluster integrity, facilitating the isolation of CTC clusters. The microchip fundamental structure unit consists of three pillars. Two pillars collaborate to form a narrow channel that separates cells, and the third pillar is placed to bifurcate the laminar flow. As blood flows through the system, individual blood cells and tumor cells direct themselves to streamlines at the bifurcation. In contrast, CTC clusters can be captured by the channel edge due to the deformation (Figure 4a).[60] This retention is caused by the dynamic force balance to maintain an equilibrium across the bifurcating pillar.[61] The chemical-free cluster chip leverages the geometries of cellular aggregates and enables the label-free isolation of CTC clusters.

Numerous teams are dedicated to optimizing and enhancing the structure and function of the device. Qin has implemented a mechanism known as the resettable cell trap (RCT) to segregate cells based on their size and deformability.[53] RCT mechanism features an adjustable hole that can be periodically cleared to prevent clogging (Figure 2b). The process of cell separation involves a three-step cycle: filtration, purging, and collection. The device can prevent channel clogging and remove white blood cells with strong shear forces generated during the purging step. Su presented a novel integrated microfluidic device for rapidly enriching CTCs automatically with high purity, leveraging the size differences between CTCs and blood cells (Figure 2d).[50] It incorporates multiple-cell trapping chambers on the microfluidic chip. Several microvalves are integrated to control the flow automatically. The CTC analysis unit, designed for CTC enrichment and identification, comprises approximately 5600 cell trapping chambers and individual pore microchannels (~10 × 8 μm) to ensure the trapping of larger cancer cells. The single-cell trapping chamber integrated into the microfluidic device offers further analysis at the molecular level. Six microvalves form a micropump in the reagent channel, delivering the required reagents from each reservoir to the CTC analysis unit, automatically enabling the entire process of CTC recovery, staining, washing, and detection. To increase throughput, Ribeiro-Samy developed a fast and efficient microfluidic cell filter for CTC enrichment (Figure 3c).[49] The cross-shaped chip, designed to capture CTCs, operates based on the size and deformability of cells and achieved an efficiency of 70%. Two chips can process 7.5 mL of the whole blood in 47 min with a purity level of 7.2%. The CROSS microdevice distributed the blood evenly across four distinct modules and processed up to 1 mL of whole blood per module. Each module is fitted with a set of prefilters and cell isolation filters. The cell filtering area in each module is formed by a single row of 700 anisotropic micropillars, each measuring 25 μm in diameter and spaced 5 μm apart. The prefilters, with gaps of 120 μm, are designed to prevent large clumps or debris. The performance of the CROSS chip was benchmarked against the gold standard CellSearch system using a sample set from metastatic colorectal cancer patients. Combined with pressure sensing, Onoshima developed a leukocyte depletion and size-based CTC enrichment device.[55] The filtration behavior in isolating tumor cells from leukocytes was experimentally investigated by using pressure sensing (Figure 3f), which demonstrated an average recovery rate exceeding 96% for spiked tumor cells and a depletion efficiency of over 99% for total leukocytes. Genomic profiling of CTCs was subsequently analyzed using the blood microfiltration device. The application of this method can further applied to DNA amplification on a limited number of microfiltered CTCs.

The integration of other functions of CTC enrichment in a microfluidic device has become one of the main focuses of the microfluidic community. Chu developed a 3D-printed device for the enrichment of CTCs from whole blood.[47] The researchers designed and fabricated a 3D microfluidic device to capture tens of millions of nonlabeled WBCs on the inner surfaces. Subsequently, it selectively removed RBCs and platelets by the size difference of the CTCs (Figure 3b). The device demonstrated an approximate 2.34-log depletion and captured over 99.5% of white blood cells from a 10 mL whole blood sample while recovering over 90% of spiked tumor cells. Xu has developed an integrated CTC enrichment platform that demonstrates high throughput and high efficiency with minimal cell damage.[52] By introducing tumor cells (PC-9) into blood samples, the device achieved a capture rate of approximately 85%, overcoming limitations of existing CTC enrichment techniques with a trade-off between purity and throughput.[62] Meanwhile, J. Wang developed an integrated device that combines spiral channel and size-based filter separation and enrichment device (Figure 3e).[63] The device incorporates a filtration system that uses a micropore-arrayed membrane and a magnetic microfluidic chip. The filtration process offers a high-throughput approach to CTC isolation and minimizes cell damage. The micropore-arrayed membrane enables precise separation of CTCs from other blood components based on size, and the subsequent magnetic microfluidic chip further improves the purification process. Han invented a hybrid apparatus that combined centrifugation and membrane filtration and utilized a horizontal rotator and fluid itself to separate and capture CTCs in a highly efficient manner (Figure 2a).[54] The device demonstrated an average capture efficiency of 95.8% for various types of cancer cells, with over 90% cell survival rate, highlighting its potential for routine detection and analysis of CTCs in clinical settings.

Kim developed a fluid-assisted separation technology (FAST) disc that features liquid-filled pores to provide gentle and more efficient filtration with diminished pressure (Figure 2e).[45,64] Using the stand-alone lab-on-a-disc system along equipped with the (FAST disc), they achieved clog-free, highly sensitive (95.9 ± 3.1% recovery rate), high selective (>2.5 log depletion of white blood cells), rapid (>3 mL/min), and label-free isolation of viable CTCs from the whole blood without prior sample preparation. Similarly, Wang has developed an integrated microfluidic system to enrich CTCs and analyze the

https://doi.org/10.1021/acsomega.4c08606
ACS Omega 2025, 10, 6306−6322

proliferation ability based on cell size to enhance metastasis prediction accuracy and eliminate the need of sample pretreatments (Figure 2f).[51]

DENSITY-BASED ENRICHMENT

Density gradient centrifugation is a widely employed technique in biomedical research for separating various cellular components within blood samples. By harnessing centrifugal force, this method capitalizes on the principles outlined in Stokes' law, where the sedimentation rate of particles is influenced by their size and density and density of the suspension fluid. As the sample undergoes centrifugation, different cell types traverse through the density gradient at distinct rates, resulting in the formation of identifiable zones within the centrifuge tubes. The denser particles, such as RBCs and neutrophils (with a density exceeding 1.077 g/mL), settle at the bottom of the centrifuge tube. In contrast, CTCs, plasma, and mononuclear cells (with a density below 1.077 g/mL) form a distinct layer at the top.[65] One of the advantages of physical methods is their ability to produce label-free, unmodified, and viable cells with shorter enrichment times. A significant challenge associated with the CTC isolation technique is the potential interference with other cells such as leukocytes. Separation of cellular components in the blood is commonly accomplished through density gradient centrifugation, which applies centrifugal force to separate cells based on variations of their sedimentation coefficients. In accordance with Stokes' law of sedimentation, the sedimentation rate of a particle is directly proportional to both size and density.[65] Heavier particles, such as RBC and neutrophils, usually settle at the bottom, whereas CTC, plasma, and mononuclear components remain at the top.[66]

Centrifugation was first utilized in 1950 by Fawcett et al. to isolate cancer cells from peritoneal fluid. The research demonstrated positive results; however, the albumin used as a flotation medium to form layers was expensive and difficult to prepare.[67] The OncoQuick technique (Grenier BioOne, Frickenhausen, Germany), tailored for CTC isolation, integrates density-based gradient centrifugation and filtration by incorporating a porous barrier into the system above the separation media and design to capture CTCs while allowing the passage of erythrocytes and leukocytes through the device.[66] OncoQuick technology represents an innovative technology incorporating a porous barrier within a 50 mL centrifuge tube, aimed at preventing mixing between the lower compartment and the blood sample before centrifugation. Post buoyant density gradient centrifugation, cells are segregated and traverse the barrier based on their distinct buoyant densities. Studies on OncoQuick showed an 87% recovery rate after centrifugation and 23% (14 out of 61) detection of patients with metastatic cancer.[68] Kecili proposed a hybrid microfluidic platform (μDACS) that uses density as a biophysical marker to sort CTCs from WBCs in blood samples.[69] The platform applies the magnetic levitation technique on a microfluidic chip to segregate cells according to their specific density ranges within continuous flow condition. The platform achieved a sorting efficiency of approximately 70% for MDA-MB-231 human breast cancer cells and U-937 human monocytes at a rapid processing speed of 1 mL/h. Campton introduced a system known as AccuCyte−CyteFinder designed for the collection, identification, and retrieval of individual CTCs from blood samples for genomic analysis. This system utilizes a density-based cell separation device (AccuCyte) to isolate nucleated cells from the blood. The sample was stained with antibodies against epithelial markers and scanned with a digital microscope (CyteFinder). The results indicated high recovery rates (90−91%) and sensitivity (over 80% for single-digit CTCs) in detecting CTCs.[70]

DIELECTROPHORESIS-BASED ENRICHMENT

Dielectrophoresis (DEP) is a phenomenon where a nonuniform electric field induces a force on a dielectric particle, such as CTCs. This phenomenon was first described by Pohl in the early 1950s in both direct current (DC) and alternating current (AC).[71] The induced force leads to manipulation, separation, or movement of the particles based on their dielectric properties. DEP is a well-known label-free technique that enables CTCs' selection and isolation without the need for physical contact or labeling, utilizing the electrical property difference between CTCs and other blood cells.[72] It enhances CTC detection by isolating rare cells based on their distinctive electrical properties.[73] However, DEP systems often encounter significant drawbacks (e.g., limited throughput), which hinder their standardization and widespread adoption.[74] In DEP, microfluidic devices are frequently used to manipulate particles or cells based on their dielectric properties.[75] Microfluidics devices, along with the electric field, are widely involved in the precise control and manipulation of fluids on the microscale, often within channels or chambers that are typically on the order of micrometers in size. Another advantage of the DEP technique is that the movement of particles is independent of the background electric field's direction, and the particle retains the same movement, with the alternating electric fields. The dipole's orientation and the induced force are impacted by polarizabilities, permittivities, and frequency of the electric field. For most of the applications of DEP on cell enrichment,[76] the cell is often considered as spherical dielectric particles with a radius R suspended in a conductive medium. The force induced on those particles is written as eq 1

$$F_{DEP} = 2\pi R^3 \varepsilon_m f_{CM} \nabla |E_{rms}|^2 \quad (1)$$

where F_{DEP} is the force induced on the dielectric particles, ∇E_{rms} is the electric field gradient, ε_m is the complex polarizability of the suspending medium, and f_{CM} is the Clausius−Mossotti (CM) function[77,78] known as the CM factor. The direction of the force induced moves either with the field gradient or against the field gradient depending on the sign and module of f_{CM} defined as eq 2

$$f_{CM} = \mathrm{Re}\left[\frac{\varepsilon_p^* - \varepsilon_m^*}{\varepsilon_p^* + 2\varepsilon_m^*}\right] \quad (2)$$

where ε_p^* and ε_m^* are the complex permittivities of the suspended object and the particles, respectively. When the real part of the CM factor is larger than 0, a positive DEP force is generated, attracting cells toward the stronger electric field. When the real part of the CM factor is less than 0, the DEP forces generated become negative, and cells are directed away from the stronger electric field. It is important to determine the permittivity of cells and frequency of the electric field to generate a DEP force on different cells for the separation, and this involves utilizing single or multishell layered models. For most applications, the single shell spherical model represents

https://doi.org/10.1021/acsomega.4c08606
ACS Omega 2025, 10, 6306−6322

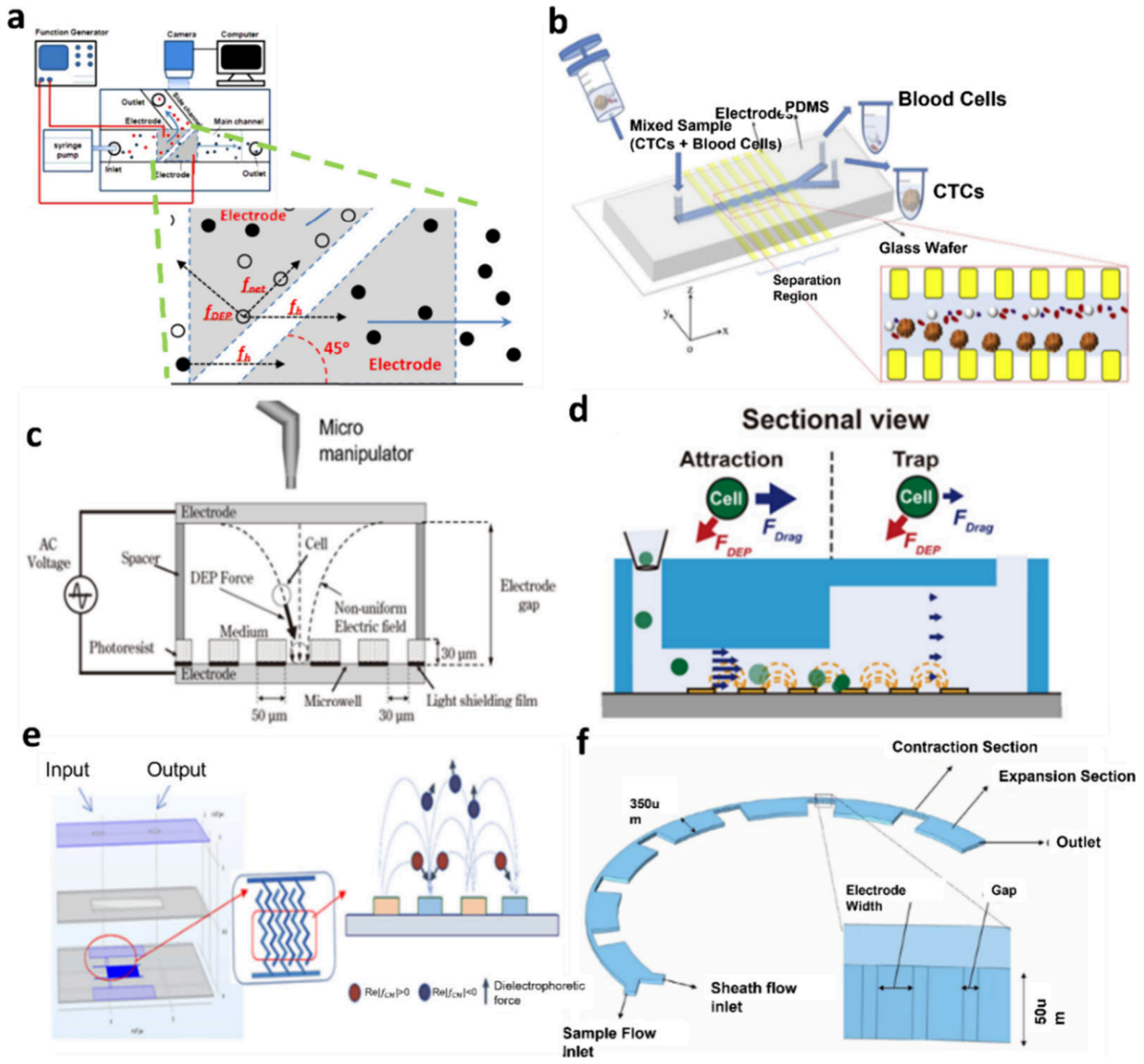

Figure 5. Example of DEP application used in microfluidics device for CTC enrichment. (a) 45° angle electrode. Reprinted with permission from ref 84. Copyright 2013, AIP Publishing. (b) LFFF-DEP. Reprinted with permission from ref 87. Copyright 2018, Elsevier. (c) High-Density Dielectrophoretic Microwell Array. Reprinted with permission from ref 90. Copyright 2023, MDPI. (d) DEP with step-channel. Reprinted with permission from ref 91. Copyright 2017, AIP Publishing. (e) DEP with zigzag interdigitated electrode. Reprinted with permission from ref 92. Copyright 2023, Elsevier. (f) DEP-based contraction−expansion inertial microfluidic channel. Reprinted with permission from ref 93. Copyright 2023, John Wiley & Sons.

cells as a spherical particle enclosed by a layer of cell membranes,[76] given by eqs 3 and 4

$$\varepsilon_p^* = \varepsilon_{mem}^* \frac{\left(\frac{R}{r}\right)^3 + 2\left(\frac{\varepsilon_{cyt}^* - \varepsilon_{mem}^*}{\varepsilon_{cyt}^* + 2\varepsilon_{mem}^*}\right)}{\left(\frac{R}{r}\right)^3 - \left(\frac{\varepsilon_{cyt}^* - \varepsilon_{mem}^*}{\varepsilon_{cyt}^* + 2\varepsilon_{mem}^*}\right)} \tag{3}$$

$$\varepsilon^* = \varepsilon + \frac{\sigma}{j\omega} \tag{4}$$

where r is the inner layer radius, ε_{cyt}^* is the complex permittivity of cell cytoplasm and ε_{mem}^* is the complex permittivity of the cell membrane, ε and σ are the permittivity and conductivity of the material, respectively, j is the imaginary unit, and ω is the angular frequency of the applied electrical field. Typically, at the crossover frequency, the DEP force and CM factor are equal to zero, and the cross-frequency should be well-defined to induce a different direction of DEP force. The efficacy of DEP cell sorting depends on the cross-frequency, which relies primarily on the dielectric properties of cells. The dielectric properties are determined by both the membrane morphology and the cytoplasm. The membrane-bound cell has its own unique dielectric properties such as surface charge and membrane capacitance, as well as the resistive properties of the membrane and cell/particle interior (cytoplasm). A nonuniform alternative electric field generates different levels of polarization between cells and determines the response of cells during DEP experiments.[79]

Alternative metallic electrode structures with diverse geometries, including interdigitated,[80] curved,[81] spiral,[82] and ring-shaped,[83] can be integrated to enhance their versatility and

https://doi.org/10.1021/acsomega.4c08606
ACS Omega 2025, 10, 6306−6322

Table 2. Summary of DEP-Based Microfluidic Techniques for CTC Enrichment

Applied voltage	Cross frequency	Medium conductivity	Cell line	Capture efficiency	Flow rate	Reference
			Continuous Flow Isolation			
10 Vpp	3 MHz		Jurkat Cell, OECM 1, HA22T	−93.5%	0.4 μL/s	98
				90.1%		
top: 10 V bottom: 15 V	Top: 10 kHz Bottom: 40 kHz	150 μS/cm	MDA-MB-231 regular blood cell	−	10 μL/h	87
9 Vpp	3.2 MHz	3000 μS/cm	MCF-7	93%	0.1 μL/min	84
			HCT-116	−		
18 Vpp	10 kHz	0.78 mS/cm	AS2-GFP	81− 85%	20 μL/min ∼2.4 mL/h	85, 86
			normal blood cell			
			Microwell Entrapment			
20 Vpp	3 MHz	300 mM mannitol solution (<200 μS/cm)	SK-BR-3	70.6−90.0%	10 cancer cells/3 mL, ∼100 cancer cells/3 mL	96
			PC-9	70.2−85.2%		
			PC-14	63.3−68.6%		
			H69	70.1−72.27%		
			SBC-3	50.2−55.9%		
			H1975	80%		
			healthy blood	−		
			HT29	75−78.2%	23 cancer cells/3 mL, 72 cancer cells/3 mL	90
			healthy blood	−		
			Continuous Flow Trapping			
20 Vpp	1 MHz	4.2 mS/m	H1975	92%	100 μL/min	91
			WBC			
80 V	65 kHz	0.055 S/m	A549	−	300 μL/min	93
			WBC			
5 V	60 kHz	150 μS/cm	MCF-7	90.41%	0.6 mL/h, ∼1.1 mL/h	92
			SMMC-7721	94.30%		
			leukocytes	−		
10 V	1 MHz	1.76 cS/m	A549	90%	0.2 μL/min	97

functionality. For example, Alshareef demonstrated the usage of a dielectrophoretic lab-on-a-chip device to efficiently separate and enrich different cancer cells.[84] Two electrodes positioned on the bottom surface of a microchannel were oriented at a 45° angle to ensure 80% of the fluid flowing through the main channel remains fluid through the side channel (Figure 5a). MCF-7 cells were guided to the side channel when applied with a negative DEP force. Cheng proposed a 3D electrode configuration to establish a long-range electric field gradient across the entire channel.[85] A negative LDEP force directed cells toward the center of the channel at the separation regions. AS2-GFP cells, subjected to a higher LDEP force, were directed more prominently toward the center into the middle subchannel. In contrast, blood cells experience a lower LDEP force, flowing to the side of the channel.[86] Waheed applied the DEP technique with Lateral Fluid Flow Fractionation (LFFF) to increase the throughput of cell enrichment using two sets of electrodes that slightly protrude into the bottom of each sidewall of the microchannel (Figure 5b).[87] When blood flows through the microchannel, all cells experience a high negative DEP (nDEP) from one set of electrodes. The frequency of another set of electrodes was adjusted in order for cancer cells to be attracted by a smaller positive DEP (pDEP) enabling the enrichment of CTC independent of cell size. However, the flow rate of the suspension medium affects the separation process, in which an increase in flow rate will decrease the time the target cell is influenced by DEP force. By leveraging the properties of magnetic nanoparticles, Labib[88] reported a unique aptamer-mediated, two-dimensional (2D) approach that isolates CTC cells with a higher level of sensitivity and specificity. The reported unique X-shaped microfabricated structures enable a low velocity and are suitable for capturing nanoparticle-tagged cells with aptamers with a high efficiency. Poudineh[89] proposed nanoparticle-mediated cell sorting by controlling the applied magnetic field along a channel as Magnetic Ranking Cytometry (MagRC), which leverages immunomagnetic separation based on CTC surface marker expression.

Meanwhile, Green[94] on the other hand proposed a new microfluidic strategy by integrating a pillar device and X-device in a series known as PillarX to efficiently capture and sort CTC clusters. The pillar device is used to separate CTC clusters from blood samples, while X-device is used to sort CTCs by exploiting magnetic nanoparticles (MNPs). Chu developed and constructed an optically induced dielectrophoresis (ODEP) microfluidic system for efficiently isolating and separating various-sized cancer cells through a two-step CTC isolation technique.[95] The blood sample was treated with negative selection-based CTC treatment to eliminate blood cells within the sample, followed by combining the ODEP cell manipulation and laminar flow to purify, separate, and sort CTCs. The ODEP system was constructed with two horizontal dynamic light image arrays and two vertical static light bar arrays. Morimoto developed a CTC enrichment capture system using a high-density dielectrophoretic microwell array. Larger cells were observed to be drawn into the microwells by

https://doi.org/10.1021/acsomega.4c08606
ACS Omega 2025, 10, 6306−6322

pDEP force more rapidly than smaller cells.[96] Utilizing a similar approach bolstered by an automated micromanipulator (Figure 5c), Nomura collected colon cancer cells from patients to conduct single-cell analysis, investigating point mutations within the KRAS, BRAF, and PIK3CA genes.[90] By changing the geometry of the microfluidics channel, Kim proposed a novel microfluidic device to significantly reduce the flow velocity within a novel step channel with increased height (Figure 5d).[91] The microfluidic device integrated an attraction zone to manage the vertical positioning of cells through the pDEP force and a trap zone to capture cells by inducing a reduction in wall shear stress and drag force. Islam proposed a microfluidics channel with a sharp change in the cross-sectional area (Figure 5f).[93] The microchannel consists of curved rectangular expansion sections and contraction sections, where the flow accelerated when entering the contraction region and decelerated when entering the expansion region. These changes in flow-induced Dean flow and lift force tended to push cells toward the center of the channel from the sidewall. The inner sidewall electrodes were needed to generate nDEP to push cells away from the trapping zone, and the process was insignificant for CTCs.

Jiang presented a three-dimensional dielectric electrophoresis microfluidic chip comprising a three-layer structure: a cover plate, a rectangular main channel, and a bottom plate with a zigzag interdigital electrode (Figure 5e).[92] Compared with conventional two-dimensional DEP microfluidic chips, the zigzag interdigital electrode is noted to provide broader electric field coverage with increased channel height, effectively addressing limitations such as low flux and elevated Joule heat. CTCs were attracted to the electrode at the chip's bottom through pDEP, while leukocytes were held in suspension in the main channel above the electrode due to nDEP. Nguyen introduced a circular microelectrode designed for the isolation, enrichment, and trapping of rare cancerous cells.[97] The circular microelectrode generated an inward-stepping electric field, and both CTCs and normal cells experienced a pDEP force. The magnitude of the DEP force acting on CTCs was significantly greater than that on red blood cells (RBCs) under the same electric field. Thus, CTCs move toward the central electrode in response to pDEP, effectively separating CTCs from normal cells. Table 2 presents a summary of DEP-based microfluidic techniques for CTC enrichment, highlighting their performance in terms of cell lines, capture efficiency, and flow rate, categorized by different mechanisms.

MICROFLUIDIC DESIGN RULE

Upon reviewing current publications on CTC enrichment devices, we analyzed the parameters of those devices, such as microchannel simulation concepts and microfabrication processes, and developed a set of design rules for future researchers to reduce design cycles and design more efficiently and economically. Simulation plays a critical role in optimizing the performance and reducing fabrication costs of a microfluidic device by early identification of design flaws. Inertial spiral microfluidic separation methods offer high throughput, label-free separation, and a simple and robust design of a microfluidic device.[99] The flow rate is one of the major parameters to consider in designing the spiral microfluidic device to achieve high purity in the outlet channel. In this paper, we conducted a targeted simulation analysis of the microfluidic device, using cited research, to establish the optimal flow rate thresholds that ensure the best performance and functioning of the device.[100−102] Figure 6 shows the design rules for the flow rate of two spiral microfluidic devices. Shiriny

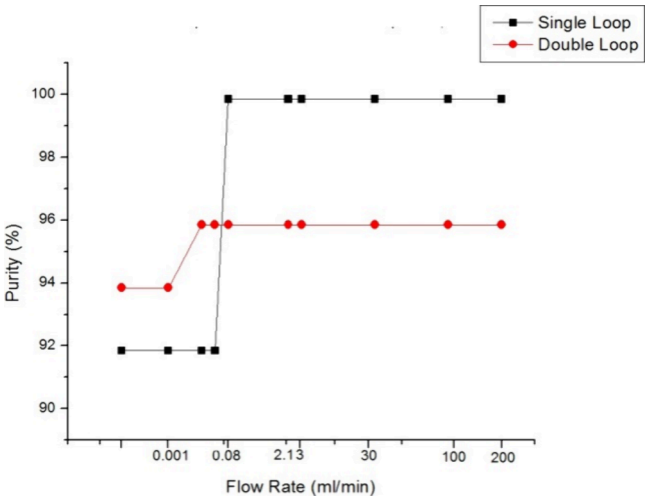

Figure 6. Flow rate of two spiral microfluidic designs for CTCs enrichment and isolation.

A. demonstrated a single-loop spiral microfluidic device for CTC (HeLa and MCF-7) enrichment and isolation.[100] They successfully isolated the CTCs with 100% separation efficiency and purity at a 2.1 mL/min flow rate. Our simulation revealed the minimum flow rate to successfully separate MCF-7 and Hela cells was 0.06 mL/min, which reduced the purity of MCF-7 to 92% (Figure 7a). Thus, flow rates below 0.06 mL/min are considered inadequate, as they significantly reduce the separation performance. The simulation and design details of the spiral microfluidic are shown in Supplementary Table 1.

Hou developed a double-loop spiral microfluidic device for CTC isolation from blood with 96% purity at a flow rate of 0.05 mL/min.[101] Based on the microfluidic dimension design developed by Hou, we redesign and perform the simulation to investigate the minimum and maximum flow rates that can affect the percentage of separation purity (Figure S1). The result in Figure 6 shows that the minimum flow rate for a double-loop spiral microfluidic device is 0.001 mL/min, and its separation purity dropped to 94%. The spiral microfluidic device applied inertial lift and Dean drag forces to different cells, which concentrated into multiple streams based on their size. This results in a state of maximum separation when the flow rate is high.[103,104] The maximum flow rate for spiral microfluidic devices was 200 mL/min, leading to leakage in microfluidic devices PDMS-based.[105−108] Spiral microfluidics devices concentrate and isolate particles and cells in the microchannel without external energy input.[109,110] Flow rate is one of the most crucial parameters to impact the inertial focusing status and the position of cells.[111,112] The simulation of minimum and maximum flow rates for spiral microfluidic devices serves as a valuable guideline for future researchers to optimize their fabrication and experimental approaches.

Another CTC enrichment and isolation technique is DLD. In DLD devices, in addition to the gap between a periodic array of micropillars, flow rate is a crucial parameter that significantly impacts their separation performance.[113] Bhattacharjee proposed a model of DLD microchannel isolating CTCs from WBCs at a flow velocity of 4.75 m/s and a separation purity of 87.7%.[114] The flow velocities of the upper

https://doi.org/10.1021/acsomega.4c08606
ACS Omega 2025, 10, 6306−6322

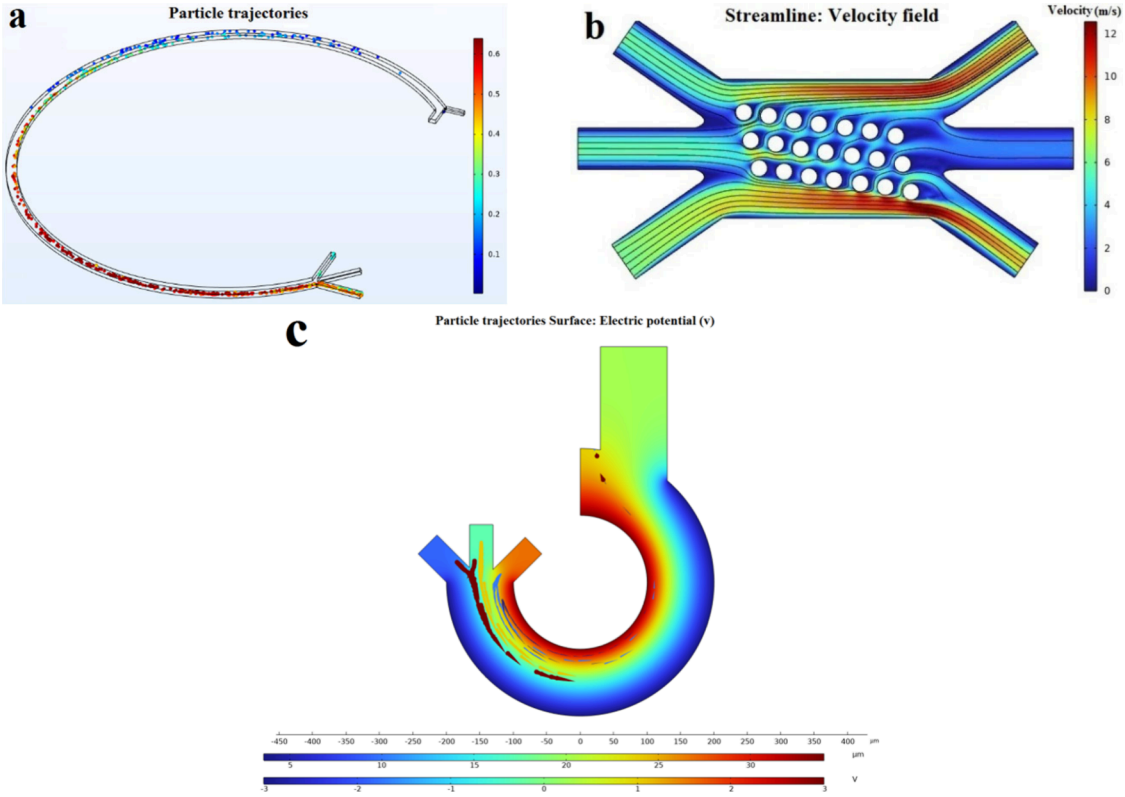

Figure 7. A simulation study of a microfluidic device for CTC enrichment and isolation based on biophysical properties. (a) Spiral microfluidic device, (b) deterministic lateral displacement (DLD) microfluidic device, and (c) dielectrophoresis (DEP).

Table 3. Design Rule for DLD Microfluidic Devices

		Reference Parameters				Design Rule							
		Velocity Flow Rate (m/s)										Velocity Flow Rate (m/s)	
ref	Cell Size (μm)	Sample	Buffer Upper	Buffer Lower	Purity (%)	Min Velocity Flow Rate of Sample (m/s)	Purity (%)	Optimum Velocity Flow Rate of Sample (m/s)	Purity (%)	Max Velocity Flow Rate of Sample (m/s)	Purity (%)	Buffer Upper	Buffer Lower
114	CTC (27), WBC (12)	12.4	4	6.7	87.5	0.05	76	0.06	81	0.65	79	0.05	0.09

Table 4. Design Rule for DEP Microfluidic Devices

		Reference Parameters				Design Rule								
						Voltage (V)			Buffer Flow Rate (mm/s)					
ref	Cell Types and Diameter (μm)	Voltage (V)	Buffer Flow Rate (mm/s)	Distance between Electrode (μm)	Purity (%)			Purity (%)			Purity (%)	Distance between Electrode (μm)		Purity (%)
115	A549 (34)	12	2.4	n/a	100	min	3	77	min	n/a	n/a	n/a		n/a
	WBC (24)					max	n/a	n/a	max	4.2	89			
	RBC (10)													
	PLT (3.6)													
118	CTC (17)	n/a	n/a	40	100	n/a		n/a	n/a		n/a	min	25	89
	WBC (12)											max	80	99
	PLT (1.8)													

buffer inlet and lower buffer inlet were maintained at 4 and 6.7 m/s, respectively. However, our simulation results showed that the flow velocities driving CTCs to exit at the upper outlet and WBCs at the middle outlet were 0.05 m/s (minimum) and 0.065 m/s (maximum) with separation purities of 76% and 79%, respectively (Figure 7b). Table 3 shows a comparison between the original setting parameters and our simulation. Meanwhile, the optimum velocity flow rate of the sample is 0.06 m/s with a purity of 81%. The velocity flow rates of the upper buffer inlet and lower buffer inlet were maintained at

https://doi.org/10.1021/acsomega.4c08606
ACS Omega 2025, 10, 6306−6322

0.05 and 0.09 m/s, respectively. As a result, there were significant differences in cell separation efficiency between our simulation results and the original findings, despite adhering to the same design parameters and operating conditions. Several factors could contribute to these discrepancies such as variations in simulation methodologies, including differences in computational models and boundary conditions. The simulation also indicated that the design separated CTCs with high purity at lower sample volume (less than 100 CTCs).

Nan developed low-frequency DEP microfluidic devices for CTC isolation with a separation purity of 100% at a buffer flow rate and voltage of 2.4 mm/s and 12 V, respectively.[115] They utilized a low-frequency band nDEP force to drive cells toward the inner channel wall with a lower electric field strength. From our simulation, the design rule is summarized in Table 4. 3 V is the minimum voltage for this device, and the purity decreased to 77% (Figure 7c). There was no significant change in purity compared to the original optimum setting when the voltage was raised to 40 V. The higher voltage may lead to a higher number of cell deaths due to a Joule heating effect.[116,117] The maximum flow velocity of 4.2 mm/s resulted in decreased separation purity from 100% to 89%. Alkhaiyat has studied a different DEP to identify the design rules.[118] They proposed a distance of 40 μm between DEP electrodes for CTC isolation to achieve 100% separation purity. Based on this design, we slightly changed the distance between electrodes to identify the minimum and maximum separation purities (Table 4). The minimum electrode distance and purity are 25 μm and 89%, respectively, and the maximum electrode distance and purity are 100 μm and 99%, respectively. As expected, the distance between electrodes plays a crucial role in determining the electric field strength and gradient, which in turn affects cell separation purity.[119] Therefore, as a result of our findings, several design rules are highlighted;

1. The optimal minimum flow rate is crucial for spiral microfluidic devices to ensure high separation purity of CTCs.
2. The precise voltage control is essential for generating effective dielectrophoretic forces required for CTC isolation.
3. The distance between electrodes must be optimized to ensure a uniform electric field distribution and effective separation.

CONCLUSION

CTCs are widely applied as biomarkers for cancer diagnosis and prognosis. Nevertheless, the examination of individual cells in CTCs is a very recent and consistently growing field that has the potential to reveal several molecular insights. These findings may serve as a foundation for early cancer detection and tracking of treatment in clinical trials. However, the analysis findings of single CTCs are still influenced by several aspects, including the very low levels, diverse biology, and susceptibility of CTCs. Creating an effective technique for isolating CTCs is critical to accomplish high throughput, purity, selectivity, and viability enrichment. Compared with traditional methods, the devices using microfluidic techniques can be cost-efficient and portable with expedited separating procedures. In this review, we focus on microfluidic devices to enrich and isolate the CTC cells based on their biophysical properties. Several microfluidic techniques, such as centrifugation, filtration, micro/nano substrates, and DLD, are reviewed and discussed. All of these techniques are based on the size and deformability of cell properties. However, other biophysical properties like density and electrical charge properties were also studied.

We also conducted simulation studies on several microfluidic designs to determine the design rules and specifications. The ideal design rules and parameters would lead to a high purity and isolation rate of CTC cells from other particles (WBC, RBC, and platelets). In conclusion, adherence to design rules is crucial for the successful fabrication and functionality of microfluidic devices. These rules ensure that the device performs as wanted, is compatible with fabrication techniques and materials, and is reliable and cost-effective. Researchers will be able to reference proposed design rules to develop microfluidic devices for consistent and reliable results. While microfluidic devices have been able to effectively isolate and enrich CTCs using several label-free techniques, none of these technologies have achieved good separation outcomes in terms of purity, separation efficiency, and throughput simultaneously. Currently, the CTC chip has significant potential for enhancing both its screening accuracy and its screening efficiency. To address this obstacle, given the inherent difficulty of achieving both accuracy and efficiency simultaneously, future microfluidic design should prioritize the realization of one particular goal. It is important to concentrate on enhancing the cell purity and cell activity of CTCs screening for fundamental scientific investigation.

In the present study, we provided several design rules of the techniques of microfluidic devices for CTC enrichment and isolation. We aimed to establish ideal design rules and parameters that yield high purity and isolation rates of CTCs from other particles, such as WBCs, RBCs, and platelets. Our findings highlighted three key design rules: flow rate, voltage, and distance between electrodes. Optimal minimum and maximum flow rates for spiral microfluidics have been identified to achieve high and lower separation purity across three designs: single, double, and triple loop of spiral microfluidic devices. For the single loop spiral microfluidic device a flow rate of 0.06 mL/min is the minimum flow rate required to successfully separate high-purity CTCs. Meanwhile, 0.001 and 0.08 mL/min are the minimum flow rates of the double and triple loops of spiral microfluidic devices, respectively. On the other hand, the flow velocities of a DLD microfluidic device are 0.05 and 0.065 m/s for the minimum and maximum, respectively. The separation purities of this minimum and maximum are 76% and 79%, respectively. For the DEP microfluidic device, we determined the impact of the electrode distance on cell separation efficiency and purity. Our simulations revealed that the minimum electrode distance of 25 μm achieved a purity of 89%. Conversely, increasing the electrode distance to a maximum of 100 μm significantly improved the purity to 99%. Meanwhile, the minimum voltage to consider for DEP microfluidic based on low-frequency band nDEP force[115] is 3 V, where the purity decreased to 77%. These findings highlight the critical role of the flow rate electrode distance and voltage in optimizing the performance of spiral, DLD, and DEP microfluidic devices.

In addition, the advancement of CTCs microfluidic devices also derives advantages from technical advancements in areas such as microelectromechanical systems (MEMS), materials science, and biomedicine. In the coming years, microfluidic technology developed for isolating and enriching CTCs in multiple stages will be combined with enhanced features to

https://doi.org/10.1021/acsomega.4c08606
ACS Omega 2025, 10, 6306−6322

reduce the limitations of the intricate sample preparation procedure. The design rules identified in our study not only advance the field of microfluidic CTC isolation but also offer significant economic and technological benefits. Optimized design parameters lead to higher purity and isolation rates of CTCs, providing a robust foundation for downstream analyses and personalized cancer treatment strategies. These advancements are crucial for early cancer detection and monitoring, potentially leading to better patient outcomes. Additionally, improved designs reduce operational costs and complexity, making CTC isolation technology more accessible and affordable for clinical and research applications. The enhanced efficiency and sensitivity of microfluidic devices can lower the overall cost of cancer diagnostics and treatment by enabling earlier and more accurate detection. Further investigation and solutions are needed prior to the practical implementation of these microfluidic devices for accurately forecasting treatment outcomes and for informing personalized medical decisions in medical practices. Looking ahead, integrating these design principles with emerging technologies, such as artificial intelligence and machine learning, could further enhance the performance and adaptability of microfluidic systems. These improvements hold great promise for transforming cancer diagnostics and treatment, ultimately contributing to more efficient healthcare solutions and better patient outcomes.

■ ASSOCIATED CONTENT

Data Availability Statement

All data generated or analyzed during this study are included in this published article.

Supporting Information

The Supporting Information is available free of charge at https://pubs.acs.org/doi/10.1021/acsomega.4c08606.

Device dimension and simulation details (PDF)

A single-loop spiral microfluidic device for CTC enrichment and isolation (MP4)

Separator microchannel structure using DEP for CTC isolation (MP4)

The curvature low-frequency DEP microfluidic separation (MP4)

■ AUTHOR INFORMATION

Corresponding Authors

Mohd Ridzuan Ahmad − *Department of Control and Mechatronics Engineering, Faculty of Electrical Engineering, Universiti Teknologi Malaysia, 81310 Skudai, Johor, Malaysia;* orcid.org/0000-0002-1331-9606; Email: mdridzuan@utm.my

Xiang Ren − *School of Microelectronics, Tianjin University, Tianjin 300072, China;* orcid.org/0000-0002-8882-6362; Email: xren@tju.edu.cn

Authors

Muhammad Asraf Mansor − *Department of Control and Mechatronics Engineering, Faculty of Electrical Engineering, Universiti Teknologi Malaysia, 81310 Skudai, Johor, Malaysia;* orcid.org/0000-0002-2711-6631

Chun Yang − *School of Microelectronics, Tianjin University, Tianjin 300072, China*

Kar Lok Chong − *Department of Control and Mechatronics Engineering, Faculty of Electrical Engineering, Universiti Teknologi Malaysia, 81310 Skudai, Johor, Malaysia*

Muhammad Asyraf Jamrus − *Department of Control and Mechatronics Engineering, Faculty of Electrical Engineering, Universiti Teknologi Malaysia, 81310 Skudai, Johor, Malaysia*

Kewei Liu − *Sino-German College of Intelligent Manufacturing, Shenzhen Technology University, Shenzhen 518118, China*

Miao Yu − *Department of Research and Development, Stedical Scientific, Carlsbad, California 92010, United States*

Complete contact information is available at: https://pubs.acs.org/10.1021/acsomega.4c08606

Author Contributions

M.A.M., C.Y., K.L.C., M.A.J., M.R.A., and X.R.: conceptualization, methodology, investigation, analysis and writing-original draft. M.A.M.: editing. M.R.A., M.Y., K.L., and X.R.: writing and revising, editing, and supervision.

Notes

The authors declare no competing financial interest.

■ ACKNOWLEDGMENTS

We would like to express our gratitude to the Ministry of Higher Education of Malaysia, Universiti Teknologi Malaysia, and Tianjin University, China, for financing this research and providing continued support. This project is supported by the Universiti Teknologi Malaysia under the Professional Development Research University Grant [Q.J130000.21A2.06E67] in the project "Development of Microfluidic Systems in PDMS for Microalgae Detection and Separation for Renewal Energy Application" and also by Natural Science Foundation of China (81903058), the startup funding and the discretionary funding (2023XJS-0035) provided by Tianjin University, and the discretionary funding JSZZ202301003 from Shenzhen Technology University.

■ REFERENCES

(1) Lin, D.; Shen, L.; Luo, M.; Zhang, K.; Li, J.; Yang, Q.; Zhu, F.; Zhou, D.; Zheng, S.; Chen, Y.; Zhou, J. Circulating Tumor Cells: Biology and Clinical Significance. *Signal Transduct Target Ther* **2021**, *6* (1), 404.

(2) Schuster, E.; Taftaf, R.; Reduzzi, C.; Albert, M. K.; Romero-Calvo, I.; Liu, H. Better Together: Circulating Tumor Cell Clustering in Metastatic Cancer. *Trends Cancer* **2021**, *7* (11), 1020−1032.

(3) Keller, L.; Pantel, K. Unravelling Tumour Heterogeneity by Single-Cell Profiling of Circulating Tumour Cells. *Nat. Rev. Cancer* **2019**, *19* (10), 553−567.

(4) Pantel, K.; Alix-Panabières, C. Liquid Biopsy and Minimal Residual Disease — Latest Advances and Implications for Cure. *Nat. Rev. Clin Oncol* **2019**, *16* (7), 409−424.

(5) Ashworth, T. R. A Case of Cancer in Which Cells Similar to Those in the Tumours Were Seen in the Blood after Death. *Med. J. Aust* **1869**, *14*, 146−147.

(6) Paterlini-Brechot, P.; Benali, N. L. Circulating Tumor Cells (CTC) Detection: Clinical Impact and Future Directions. *Cancer Lett.* **2007**, *253* (2), 180−204.

(7) Natalia, A.; Zhang, L.; Sundah, N. R.; Zhang, Y.; Shao, H. Analytical Device Miniaturization for the Detection of Circulating Biomarkers. *Nature Reviews Bioengineering* **2023**, *1* (July), 481.

(8) Akpe, V.; Kim, T. H.; Brown, C. L.; Cock, I. E. Circulating Tumour Cells: A Broad Perspective. *J. R Soc. Interface* **2020**, *17* (168), 20200065.

(9) Hong, Y.; Fang, F.; Zhang, Q. Circulating Tumor Cell Clusters: What We Know and What We Expect (Review). *Int. J. Oncol.* **2016**, *49* (6), 2206−2216.

(10) Aceto, N.; Bardia, A.; Miyamoto, D. T.; Donaldson, M. C.; Wittner, B. S.; Spencer, J. A.; Yu, M.; Pely, A.; Engstrom, A.; Zhu, H.; Brannigan, B. W.; Kapur, R.; Stott, S. L.; Shioda, T.; Ramaswamy, S.; Ting, D. T.; Lin, C. P.; Toner, M.; Haber, D. A.; Maheswaran, S. Circulating Tumor Cell Clusters Are Oligoclonal Precursors of Breast Cancer Metastasis. *Cell* **2014**, *158* (5), 1110−1122.
(11) Liu, X.; Taftaf, R.; Kawaguchi, M.; Chang, Y.-F.; Chen, W.; Entenberg, D.; Zhang, Y.; Gerratana, L.; Huang, S.; Patel, D. B.; Tsui, E.; Adorno-Cruz, V.; Chirieleison, S. M.; Cao, Y.; Harney, A. S.; Patel, S.; Patsialou, A.; Shen, Y.; Avril, S.; Gilmore, H. L.; Lathia, J. D.; Abbott, D. W.; Cristofanilli, M.; Condeelis, J. S.; Liu, H. Homophilic CD44 Interactions Mediate Tumor Cell Aggregation and Polyclonal Metastasis in Patient-Derived Breast Cancer Models. *Cancer Discov* **2019**, *9* (1), 96−113.
(12) Shanehband, N.; Naghib, S. M. Recent Advances in Nano/Microfluidics-Based Cell Isolation Techniques for Cancer Diagnosis and Treatments. *Biochimie* **2024**, *220*, 122−143.
(13) Qian, W.; Zhang, Y.; Chen, W. Capturing Cancer: Emerging Microfluidic Technologies for the Capture and Characterization of Circulating Tumor Cells. *Small* **2015**, *11* (32), 3850−3872.
(14) Wills, Q. F.; Mead, A. J. Application of Single-Cell Genomics in Cancer: Promise and Challenges. *Hum. Mol. Genet.* **2015**, *24* (R1), R74−R84.
(15) Mansor, M. A.; Ahmad, M. R. Single Cell Electrical Characterization Techniques. *Int. J. Mol. Sci.* **2015**, *16* (6), 12686−12712.
(16) Mostert, B.; Sleijfer, S.; Foekens, J. A.; Gratama, J. W. Circulating Tumor Cells (CTCs): Detection Methods and Their Clinical Relevance in Breast Cancer. *Cancer Treat Rev.* **2009**, *35* (5), 463−474.
(17) Lalmahomed, Z. S.; Kraan, J.; Gratama, J. W.; Mostert, B.; Sleijfer, S.; Verhoef, C. Circulating Tumor Cells and Sample Size: The More, the Better. *Journal of Clinical Oncology* **2010**, *28* (17), e288−e289.
(18) Yang, Z. F.; Ngai, P.; Ho, D. W.; Yu, W. C.; Ng, M. N.P.; Lau, C. K.; Li, M. L. Y.; Tam, K. H.; Lam, C. T.; Poon, R. T. P.; Fan, S. T. Identification of Local and Circulating Cancer Stem Cells in Human Liver Cancer. *Hepatology* **2008**, *47* (3), 919−928.
(19) Gertler, R.; Rosenberg, R.; Fuehrer, K.; Dahm, M.; Nekarda, H.; Siewert, J. R. *Detection of Circulating Tumor Cells in Blood Using an Optimized Density Gradient Centrifugation* **2003**, *162*, 149−155.
(20) Hou, H. W.; Petchakup, C.; Tay, H. M.; Tam, Z. Y.; Dalan, R.; Chew, D. E. K.; Li, K. H. H.; Boehm, B. O. Rapid and Label-Free Microfluidic Neutrophil Purification and Phenotyping in Diabetes Mellitus. *Sci. Rep.* **2016**, *6*, 1−12.
(21) Söderström, A. C.; Nybo, M.; Nielsen, C.; Vinholt, P. J. The Effect of Centrifugation Speed and Time on Pre-Analytical Platelet Activation. *Clinical Chemistry and Laboratory Medicine (CCLM)* **2016**, *54* (12), 1913−1920.
(22) S. Iliescu, F.; Sim, W. J.; Heidari, H.; P. Poenar, D.; Miao, J.; Taylor, H. K.; Iliescu, C. Highlighting the Uniqueness in Dielectrophoretic Enrichment of Circulating Tumor Cells. *Electrophoresis* **2019**, *40* (10), 1457−1477.
(23) Marrinucci, D.; Bethel, K.; Kolatkar, A.; Luttgen, M. S.; Malchiodi, M.; Baehring, F.; Voigt, K.; Lazar, D.; Nieva, J.; Bazhenova, L.; Ko, A. H.; Korn, W. M.; Schram, E.; Coward, M.; Yang, X.; Metzner, T.; Lamy, R.; Honnatti, M.; Yoshioka, C.; Kunken, J.; Petrova, Y.; Sok, D.; Nelson, D.; Kuhn, P. Fluid Biopsy in Patients with Metastatic Prostate, Pancreatic and Breast Cancers. *Phys. Biol.* **2012**, *9* (1), No. 016003.
(24) Kalluri, R. EMT: When Epithelial Cells Decide to Become Mesenchymal-like Cells. *J. Clin. Invest.* **2009**, *119* (6), 1417−1419.
(25) Arya, S. K.; Lim, B.; Rahman, A. R. A. Enrichment, Detection and Clinical Significance of Circulating Tumor Cells. *Lab Chip* **2013**, *13* (11), 1995−2027.
(26) Li, X.; Li, Y.; Shao, W.; Li, Z.; Zhao, R.; Ye, Z. Strategies for Enrichment of Circulating Tumor Cells. *Transl Cancer Res.* **2020**, *9* (3), 2012−2025.
(27) Mansor, M. A.; Jamrus, M. A.; Lok, C. K.; Ahmad, M. R.; Petrů, M.; Koloor, S. S. R. Microfluidic Device for Both Active and Passive Cell Separation Techniques: A Review. *Sensors and Actuators Reports* **2025**, *9*, 100277.
(28) Song, Y.; Tian, T.; Shi, Y.; Liu, W.; Zou, Y.; Khajvand, T.; Wang, S.; Zhu, Z.; Yang, C. Enrichment and Single-Cell Analysis of Circulating Tumor Cells. *Chem. Sci.* **2017**, *8* (3), 1736−1751.
(29) Ju, S.; Chen, C.; Zhang, J.; Xu, L.; Zhang, X.; Li, Z.; Chen, Y.; Zhou, J.; Ji, F.; Wang, L. Detection of Circulating Tumor Cells: Opportunities and Challenges. *Biomark Res.* **2022**, *10* (1), 1−25.
(30) Rushton, A. J.; Nteliopoulos, G.; Shaw, J. A.; Coombes, R. C. A Review of Circulating Tumour Cell Enrichment Technologies. *Cancers (Basel)* **2021**, *13* (5), 970.
(31) Farahinia, A.; Zhang, W.; Badea, I. Recent Developments in Inertial and Centrifugal Microfluidic Systems along with the Involved Forces for Cancer Cell Separation: A Review. *Sensors* **2023**, *23* (11), 5300.
(32) Wu, F.; Kong, X.; Liu, Y.; Wang, S.; Chen, Z.; Hou, X. Microfluidic-Based Isolation of Circulating Tumor Cells with High-Efficiency and High-Purity. *Chin. Chem. Lett.* **2024**, *35* (8), No. 109754.
(33) Enders, A.; Grünberger, A.; Bahnemann, J. Towards Small Scale: Overview and Applications of Microfluidics in Biotechnology. *Mol. Biotechnol* **2024**, *66* (3), 365−377.
(34) Vidlarova, M.; Rehulkova, A.; Stejskal, P.; Prokopova, A.; Slavik, H.; Hajduch, M.; Srovnal, J. Recent Advances in Methods for Circulating Tumor Cell Detection. *Int. J. Mol. Sci.* **2023**, *24* (4), 3902.
(35) Feng, J.; Mo, J.; Zhang, A.; Liu, D.; Zhou, L.; Hang, T.; Yang, C.; Wu, Q.; Xia, D.; Wen, R.; Yang, J.; Feng, Y.; Huang, Y.; Hu, N.; He, G.; Xie, X. Antibody-Free Isolation and Regulation of Adherent Cancer Cells: Via Hybrid Branched Microtube-Sandwiched Hydrodynamic System. *Nanoscale* **2020**, *12* (8), 5103−5113.
(36) Fan, X.; Jia, C.; Yang, J.; Li, G.; Mao, H.; Jin, Q.; Zhao, J. A Microfluidic Chip Integrated with a High-Density PDMS-Based Microfiltration Membrane for Rapid Isolation and Detection of Circulating Tumor Cells. *Biosens Bioelectron* **2015**, *71*, 380−386.
(37) Ferreira, M. M.; Ramani, V. C.; Jeffrey, S. S. Circulating Tumor Cell Technologies. *Mol. Oncol* **2016**, *10* (3), 374−394.
(38) Hao, S.-J.; Wan, Y.; Xia, Y.-Q.; Zou, X.; Zheng, S.-Y. Size-Based Separation Methods of Circulating Tumor Cells. *Adv. Drug Deliv Rev.* **2018**, *125*, 3−20.
(39) Hosokawa, M.; Yoshikawa, T.; Negishi, R.; Yoshino, T.; Koh, Y.; Kenmotsu, H.; Naito, T.; Takahashi, T.; Yamamoto, N.; Kikuhara, Y.; Kanbara, H.; Tanaka, T.; Yamaguchi, K.; Matsunaga, T. Microcavity Array System for Size-Based Enrichment of Circulating Tumor Cells from the Blood of Patients with Small-Cell Lung Cancer. *Anal. Chem.* **2013**, *85* (12), 5692−5698.
(40) Hosokawa, M.; Hayata, T.; Fukuda, Y.; Arakaki, A.; Yoshino, T.; Tanaka, T.; Matsunaga, T. Size-Selective Microcavity Array for Rapid and Efficient Detection of Circulating Tumor Cells. *Anal. Chem.* **2010**, *82* (15), 6629−6635.
(41) Zhang, S.; Wang, Y.; Yang, C.; Zhu, J.; Ye, X.; Wang, W. On-Chip Circulating Tumor Cells Isolation Based on Membrane Filtration and Immuno-Magnetic Bead Clump Capture. *Nanotechnology and Precision Engineering* **2022**, *5* (1), 013003.
(42) Meunier, A.; Hernández-Castro, J. A.; Turner, K.; Li, K.; Veres, T.; Juncker, D. Combination of Mechanical and Molecular Filtration for Enhanced Enrichment of Circulating Tumor Cells. *Anal. Chem.* **2016**, *88* (17), 8510−8517.
(43) Karlsson, J. M.; Haraldsson, T.; Carlborg, C. F.; Hansson, J.; Russom, A.; van der Wijngaart, W. Fabrication and Transfer of Fragile 3D PDMS Microstructures. *Journal of Micromechanics and Microengineering* **2012**, *22* (8), No. 085009.
(44) Kihara, N.; Kuboyama, D.; Onoshima, D.; Ishikawa, K.; Tanaka, H.; Ozawa, N.; Hase, T.; Koguchi, R.; Yukawa, H.; Odaka, H.; Hasegawa, Y.; Baba, Y.; Hori, M. Low-Autofluorescence Fluoropolymer Membrane Filters for Cell Filtration. *Jpn. J. Appl. Phys.* **2018**, *57*, 06JF03.

https://doi.org/10.1021/acsomega.4c08606
ACS Omega 2025, 10, 6306−6322

(45) Kim, T.-H.; Lim, M.; Park, J.; Oh, J. M.; Kim, H.; Jeong, H.; Lee, S. J.; Park, H. C.; Jung, S.; Kim, B. C.; Lee, K.; Kim, M.-H.; Park, D. Y.; Kim, G. H.; Cho, Y.-K. FAST: Size-Selective, Clog-Free Isolation of Rare Cancer Cells from Whole Blood at a Liquid−Liquid Interface. *Anal. Chem.* **2017**, *89* (2), 1155−1162.
(46) Huang, T.; Jia, C.-P.; Jun-Yang; Sun, W.-J.; Wang, W.-T.; Zhang, H.-L.; Cong, H.; Jing, F.-X.; Mao, H.-J.; Jin, Q.-H.; Zhang, Z.; Chen, Y.-J.; Li, G.; Mao, G.-X.; Zhao, J.-L. Highly Sensitive Enumeration of Circulating Tumor Cells in Lung Cancer Patients Using a Size-Based Filtration Microfluidic Chip. *Biosens Bioelectron* **2014**, *51*, 213−218.
(47) Chu, C. H.; Liu, R.; Ozkaya-Ahmadov, T.; Swain, B. E.; Boya, M.; El-Rayes, B.; Akce, M.; Bilen, M. A.; Kucuk, O.; Sarioglu, A. F. Negative Enrichment of Circulating Tumor Cells from Unmanipulated Whole Blood with a 3D Printed Device. *Sci. Rep* **2021**, *11* (1), 1−12.
(48) Zhou, M.-D.; Hao, S.; Williams, A. J.; Harouaka, R. A.; Schrand, B.; Rawal, S.; Ao, Z.; Brenneman, R.; Gilboa, E.; Lu, B.; Wang, S.; Zhu, J.; Datar, R.; Cote, R.; Tai, Y.-C.; Zheng, S.-Y. Separable Bilayer Microfiltration Device for Viable Label-Free Enrichment of Circulating Tumour Cells. *Sci. Rep* **2014**, *4* (1), 7392.
(49) Ribeiro-Samy, S.; Oliveira, M. I.; Pereira-Veiga, T.; Muinelo-Romay, L.; Carvalho, S.; Gaspar, J.; Freitas, P. P.; López-López, R.; Costa, C.; Diéguez, L. Fast and Efficient Microfluidic Cell Filter for Isolation of Circulating Tumor Cells from Unprocessed Whole Blood of Colorectal Cancer Patients. *Sci. Rep* **2019**, *9* (1), 1−12.
(50) Su, W.; Yu, H.; Jiang, L.; Chen, W.; Li, H.; Qin, J. Integrated Microfluidic Device for Enrichment and Identification of Circulating Tumor Cells from the Blood of Patients with Colorectal Cancer. *Dis Markers* **2019**, *2019*, 1.
(51) Wang, J.; Meng, X.; Yu, M.; Li, X.; Chen, Z.; Wang, R.; Fang, J. A Novel Microfluidic System for Enrichment of Functional Circulating Tumor Cells in Cancer Patient Blood Samples by Combining Cell Size and Invasiveness. *Biosens Bioelectron* **2023**, *227*, No. 115159.
(52) Xu, M.; Liu, W.; Zou, K.; Wei, S.; Zhang, X.; Li, E.; Wang, Q. Design and Clinical Application of an Integrated Microfluidic Device for Circulating Tumor Cells Isolation and Single-Cell Analysis. *Micromachines (Basel)* **2021**, *12* (1), 49.
(53) Qin, X.; Park, S.; Duffy, S. P.; Matthews, K.; Ang, R. R.; Todenhöfer, T.; Abdi, H.; Azad, A.; Bazov, J.; Chi, K. N.; Black, P. C.; Ma, H. Size and Deformability Based Separation of Circulating Tumor Cells from Castrate Resistant Prostate Cancer Patients Using Resettable Cell Traps. *Lab Chip* **2015**, *15* (10), 2278−2286.
(54) Han, J.; Lu, C.; Shen, M.; Sun, X.; Mo, X.; Yang, G. Fast, Reusable, Cell Uniformly Distributed Membrane Filtration Device for Separation of Circulating Tumor Cells. *ACS Omega* **2022**, *7* (24), 20761−20767.
(55) Onoshima, D.; Hase, T.; Kihara, N.; Kuboyama, D.; Tanaka, H.; Ozawa, N.; Yukawa, H.; Sato, M.; Ishikawa, K.; Hasegawa, Y.; Ishii, M.; Hori, M.; Baba, Y. Leukocyte Depletion and Size-Based Enrichment of Circulating Tumor Cells Using a Pressure-Sensing Microfiltration Device. *ACS Measurement Science Au* **2023**, *3* (2), 113−119.
(56) Sarioglu, A. F.; Aceto, N.; Kojic, N.; Donaldson, M. C.; Zeinali, M.; Hamza, B.; Engstrom, A.; Zhu, H.; Sundaresan, T. K.; Miyamoto, D. T.; Luo, X.; Bardia, A.; Wittner, B. S.; Ramaswamy, S.; Shioda, T.; Ting, D. T.; Stott, S. L.; Kapur, R.; Maheswaran, S.; Haber, D. A.; Toner, M. A Microfluidic Device for Label-Free, Physical Capture of Circulating Tumor Cell Clusters. *Nat. Methods* **2015**, *12* (7), 685−691.
(57) Yee-de León, J. F.; Soto-García, B.; Aráiz-Hernández, D.; Delgado-Balderas, J. R.; Esparza, M.; Aguilar-Avelar, C.; Wong-Campos, J. D.; Chacón, F.; López-Hernández, J. Y.; González-Treviño, A. M.; Yee-de León, J. R.; Zamora-Mendoza, J. L.; Alvarez, M. M.; Trujillo-de Santiago, G.; Gómez-Guerra, L. S.; Sánchez-Domínguez, C. N.; Velarde-Calvillo, L. P.; Abarca-Blanco, A. Characterization of a Novel Automated Microfiltration Device for the Efficient Isolation and Analysis of Circulating Tumor Cells from Clinical Blood Samples. *Sci. Rep* **2020**, *10* (1), 1−12.
(58) Li, H.; Li, J.; Zhang, Z.; Guo, Z.; Zhang, C.; Wang, Z.; Guo, Q.; Li, C.; Li, C.; Yao, J.; Zheng, A.; Xu, J.; Gao, Q.; Zhang, W.; Zhou, L. Integrated Microdevice with a Windmill-like Hole Array for the Clog-Free, Efficient, and Self-Mixing Enrichment of Circulating Tumor Cells. *Microsyst Nanoeng* **2022**, *8* (1), 23.
(59) Zhou, M.; Hao, S.; Williams, A. J.; Harouaka, R. A.; Schrand, B.; Rawal, S.; Ao, Z.; Brenneman, R.; Gilboa, E.; Lu, B.; Wang, S.; Zhu, J.; Datar, R.; Cote, R.; Tai, Y. C.; Zheng, S. Y. Separable Bilayer Microfiltration Device for Viable Label-Free Enrichment of Circulating Tumour Cells. *Sci. Rep* **2014**, *4*, 7392.
(60) Mong, J.; Tan, M.-H. Size-Based Enrichment Technologies for Non-Cancerous Tumor-Derived Cells in Blood. *Trends Biotechnol* **2018**, *36* (5), 511−522.
(61) Coumans, F. A. W.; van Dalum, G.; Beck, M.; Terstappen, L. W. M. M. Filter Characteristics Influencing Circulating Tumor Cell Enrichment from Whole Blood. *PLoS One* **2013**, *8* (4), e61770.
(62) Liu, Y.; Li, T.; Xu, M.; Zhang, W.; Xiong, Y.; Nie, L.; Wang, Q.; Li, H.; Wang, W. A High-Throughput Liquid Biopsy for Rapid Rare Cell Separation from Large-Volume Samples. *Lab Chip* **2019**, *19* (1), 68−78.
(63) Wang, J.; Lu, W.; Tang, C.; Liu, Y.; Sun, J.; Mu, X.; Zhang, L.; Dai, B.; Li, X.; Zhuo, H.; Jiang, X. Label-Free Isolation and MRNA Detection of Circulating Tumor Cells from Patients with Metastatic Lung Cancer for Disease Diagnosis and Monitoring Therapeutic Efficacy. *Anal. Chem.* **2015**, *87* (23), 11893−11900.
(64) Gorkin, R.; Park, J.; Siegrist, J.; Amasia, M.; Lee, B. S.; Park, J.-M.; Kim, J.; Kim, H.; Madou, M.; Cho, Y.-K. Centrifugal Microfluidics for Biomedical Applications. *Lab Chip* **2010**, *10* (14), 1758.
(65) Low, W. S.; Wan Abas, W. A. B. Benchtop Technologies for Circulating Tumor Cells Separation Based on Biophysical Properties. *Biomed Res. Int.* **2015**, *2015*, 1.
(66) Rosenberg, R.; Gertler, R.; Friederichs, J.; Fuehrer, K.; Dahm, M.; Phelps, R.; Thorban, S.; Nekarda, H.; Siewert, J. R. *Comparison of Two Density* Gradient Centrifugation Systems for the Enrichment of Disseminated Tumor Cells in Blood. *Cytometry* **2002**, *49* (4), 150−158.
(67) Fawcett, D. W.; Vallee, B. L.; Soule, M. H. A Method for Concentration and Segregation of Malignant Cells from Bloody, Pleural, and Peritoneal Fluids. *Science (1979)* **1950**, *111* (2872), 34−36.
(68) Balic, M.; Dandachi, N.; Hofmann, G.; Samonigg, H.; Loibner, H.; Obwaller, A.; van der Kooi, A.; Tibbe, A. G. J.; Doyle, G. V.; Terstappen, L. W. M. M.; Bauernhofer, T. Comparison of Two Methods for Enumerating Circulating Tumor Cells in Carcinoma Patients. *Cytometry B Clin Cytom* **2005**, *68B* (1), 25−30.
(69) Kecili, S.; Yilmaz, E.; Ozcelik, O. S.; Anil-Inevi, M.; Gunyuz, Z. E.; Yalcin-Ozuysal, O.; Ozcivici, E.; Tekin, H. C. MDACS Platform: A Hybrid Microfluidic Platform Using Magnetic Levitation Technique and Integrating Magnetic, Gravitational, and Drag Forces for Density-Based Rare Cancer Cell Sorting. *Biosens Bioelectron X* **2023**, *15*, 1−8.
(70) Campton, D. E.; Ramirez, A. B.; Nordberg, J. J.; Drovetto, N.; Clein, A. C.; Varshavskaya, P.; Friemel, B. H.; Quarre, S.; Breman, A.; Dorschner, M.; Blau, S.; Blau, C. A.; Sabath, D. E.; Stilwell, J. L.; Kaldjian, E. P. High-Recovery Visual Identification and Single-Cell Retrieval of Circulating Tumor Cells for Genomic Analysis Using a Dual-Technology Platform Integrated with Automated Immunofluorescence Staining. *BMC Cancer* **2015**, *15* (1), 1−13.
(71) Pohl, H. A. The Motion and Precipitation of Suspensoids in Divergent Electric Fields. *J. Appl. Phys.* **1951**, *22* (7), 869−871.
(72) Ramirez-Murillo, C. J.; de los Santos-Ramirez, J. M.; Perez-Gonzalez, V. H. Toward Low-voltage Dielectrophoresis-based Microfluidic Systems: A Review. *Electrophoresis* **2021**, *42* (5), 565−587.
(73) Camarda, M.; Fisicaro, G.; Anzalone, R.; Scalese, S.; Alberti, A.; La Via, F.; La Magna, A.; Ballo, A.; Giustolisi, G.; Minafra, L.; Cammarata, F. P.; Bravatà, V.; Forte, G. I.; Russo, G.; Gilardi, M. C. Theoretical and Experimental Study of the Role of Cell-Cell Dipole

https://doi.org/10.1021/acsomega.4c08606
ACS Omega 2025, 10, 6306−6322

Interaction in Dielectrophoretic Devices: Application to Polynomial Electrodes. *Biomed Eng. Online* **2014**, *13* (1), 71.
(74) Russo, G. I.; Musso, N.; Romano, A.; Caruso, G.; Petralia, S.; Lanzanò, L.; Broggi, G.; Camarda, M. The Role of Dielectrophoresis for Cancer Diagnosis and Prognosis. *Cancers (Basel)* **2022**, *14* (1), 198.
(75) Varmazyari, V.; Ghafoorifard, H.; Habibiyan, H.; Ebrahimi, M.; Ghafouri-Fard, S. A Microfluidic Device for Label-Free Separation Sensitivity Enhancement of Circulating Tumor Cells of Various and Similar Size. *J. Mol. Liq.* **2022**, *349*, No. 118192.
(76) Gabriel, C. The Dielectric Properties of Biological Materials. In *Radiofrequency Radiation Standards*; Springer US: 1995; pp 187−196. DOI: 10.1007/978-1-4899-0945-9_20.
(77) Gascoyne, P. R. C.; Noshari, J.; Anderson, T. J.; Becker, F. F. Isolation of Rare Cells from Cell Mixtures by Dielectrophoresis. *Electrophoresis* **2009**, *30* (8), 1388−1398.
(78) Shen, Y.; Elele, E.; Khusid, B. A Novel Concept of Dielectrophoretic Engine Oil Filter. *Electrophoresis* **2011**, *32* (18), 2559−2568.
(79) Coley, H. M.; Labeed, F. H.; Thomas, H.; Hughes, M. P. Biophysical Characterization of MDR Breast Cancer Cell Lines Reveals the Cytoplasm Is Critical in Determining Drug Sensitivity. *Biochim. Biophys. Acta* **2007**, *1770* (4), 601−608.
(80) Gascoyne, P. R. C.; Wang, X. B.; Huang, Y.; Becker, R. F. Dielectrophoretic Separation of Cancer Cells from Blood. *IEEE Trans Ind. Appl.* **1997**, *33* (3), 670−678.
(81) Moon, H. S.; Kwon, K.; Kim, S.; Han, H.; Sohn, J.; Lee, S.; Jung, H. Continuous Separation of Breast Cancer Cells from Blood Samples Using Multi-Orifice Flow Fractionation (MOFF) and Dielectrophoresis (DEP). *Lab on a Chip* **2011**, *11*, 1118−1125.
(82) Menachery, A.; Kremer, C.; Wong, P. E.; Carlsson, A.; Neale, S. L.; Barrett, M. P.; Cooper, J. M. Counterflow Dielectrophoresis for Trypanosome Enrichment and Detection in Blood. *Sci. Rep* **2012**, *2*, 775.
(83) Xing, X.; Zhang, M.; Yobas, L. Interdigitated 3-D Silicon Ring Microelectrodes for DEP-Based Particle Manipulation. *Journal of Microelectromechanical Systems* **2013**, *22* (2), 363−371.
(84) Alshareef, M.; Metrakos, N.; Juarez Perez, E.; Azer, F.; Yang, F.; Yang, X.; Wang, G. Separation of Tumor Cells with Dielectrophoresis-Based Microfluidic Chip. *Biomicrofluidics* **2013**, *7* (1), 11803.
(85) Cheng, I.; Chen, T.; Lin, Y.; Huang, W.-L.; Liu, C.; Su, W. A Novel Dielectrophoresis-Based Microfluidic Chip for Antibody-Free Isolation of Circulating Tumor Cells from Blood. In *2015 IEEE 15th International Conference on Nanotechnology (IEEE-NANO)*; IEEE: 2015; pp 1525−1527. DOI: 10.1109/NANO.2015.7388934.
(86) Cheng, I. F.; Huang, W. L.; Chen, T. Y.; Liu, C. W.; Lin, Y. De; Su, W. C. Antibody-Free Isolation of Rare Cancer Cells from Blood Based on 3D Lateral Dielectrophoresis. *Lab Chip* **2015**, *15* (14), 2950−2959.
(87) Waheed, W.; Alazzam, A.; Mathew, B.; Christoforou, N.; Abu-Nada, E. Lateral Fluid Flow Fractionation Using Dielectrophoresis (LFFF-DEP) for Size-Independent, Label-Free Isolation of Circulating Tumor Cells. *Journal of Chromatography B* **2018**, *1087-1088*, 133−137.
(88) Labib, M.; Green, B.; Mohamadi, R. M.; Mepham, A.; Ahmed, S. U.; Mahmoudian, L.; Chang, I.-H.; Sargent, E. H.; Kelley, S. O. Aptamer and Antisense-Mediated Two-Dimensional Isolation of Specific Cancer Cell Subpopulations. *J. Am. Chem. Soc.* **2016**, *138* (8), 2476−2479.
(89) Poudineh, M.; Aldridge, P. M.; Ahmed, S.; Green, B. J.; Kermanshah, L.; Nguyen, V.; Tu, C.; Mohamadi, R. M.; Nam, R. K.; Hansen, A.; Sridhar, S. S.; Finelli, A.; Fleshner, N. E.; Joshua, A. M.; Sargent, E. H.; Kelley, S. O. Tracking the Dynamics of Circulating Tumour Cell Phenotypes Using Nanoparticle-Mediated Magnetic Ranking. *Nat. Nanotechnol* **2017**, *12* (3), 274−281.
(90) Nomura, M.; Miyake, Y.; Inoue, A.; Yokoyama, Y.; Noda, N.; Kouda, S.; Hata, T.; Ogino, T.; Miyoshi, N.; Takahashi, H.; Uemura, M.; Mizushima, T.; Doki, Y.; Eguchi, H.; Yamamoto, H. Single-Cell Analysis of Circulating Tumor Cells from Patients with Colorectal Cancer Captured with a Dielectrophoresis-Based Micropore System. *Biomedicines* **2023**, *11* (1), 203.
(91) Kim, S. H.; Ito, H.; Kozuka, M.; Hirai, M.; Fujii, T. Localization of Low-Abundant Cancer Cells in a Sharply Expanded Microfluidic Step-Channel Using Dielectrophoresis. *Biomicrofluidics* **2017**, *11* (5), 054114.
(92) Jiang, L.; Liang, F.; Huo, M.; Ju, M.; Xu, J.; Ju, S.; Jin, L.; Shen, B. Study on Three-Dimensional Dielectrophoresis Microfluidic Chip for Separation and Enrichment of Circulating Tumor Cells. *Microelectron. Eng.* **2023**, *282*, No. 112100.
(93) Islam, M. S.; Chen, X. Continuous CTC Separation through a DEP-Based Contraction−Expansion Inertial Microfluidic Channel. *Biotechnol. Prog.* **2023**, *39*, 1−15. No. November
(94) Green, B. J.; Marazzini, M.; Hershey, B.; Fardin, A.; Li, Q.; Wang, Z.; Giangreco, G.; Pisati, F.; Marchesi, S.; Disanza, A.; Frittoli, E.; Martini, E.; Magni, S.; Beznoussenko, G. V.; Vernieri, C.; Lobefaro, R.; Parazzoli, D.; Maiuri, P.; Havas, K.; Labib, M.; Sigismund, S.; Fiore, P. P. Di; Gunby, R. H.; Kelley, S. O.; Scita, G. PillarX: A Microfluidic Device to Profile Circulating Tumor Cell Clusters Based on Geometry, Deformability, and Epithelial State. *Small* **2022**, *18* (17), 2106097.
(95) Chu, P.-Y.; Nguyen, T. N. A.; Wu, A.-Y.; Huang, P.-S.; Huang, K.-L.; Liao, C.-J.; Hsieh, C.-H.; Wu, M.-H. The Utilization of Optically Induced Dielectrophoresis (ODEP)-Based Cell Manipulation in a Microfluidic System for the Purification and Sorting of Circulating Tumor Cells (CTCs) with Different Sizes. *Micromachines (Basel)* **2023**, *14* (12), 2170.
(96) Morimoto, A.; Mogami, T.; Watanabe, M.; Iijima, K.; Akiyama, Y.; Katayama, K.; Futami, T.; Yamamoto, N.; Sawada, T.; Koizumi, F.; Koh, Y. High-Density Dielectrophoretic Microwell Array for Detection, Capture, and Single-Cell Analysis of Rare Tumor Cells in Peripheral Blood. *PLoS One* **2015**, *10* (6), No. e0130418.
(97) Nguyen, N. V.; Jen, C. P. Impedance Detection Integrated with Dielectrophoresis Enrichment Platform for Lung Circulating Tumor Cells in a Microfluidic Channel. *Biosens Bioelectron* **2018**, *121*, 10−18.
(98) Chou, W.-P.; Wang, H.-M.; Chang, J.-H.; Chiu, T.-K.; Hsieh, C.-H.; Liao, C.-J.; Wu, M.-H. The Utilization of Optically-Induced-Dielectrophoresis (ODEP)-Based Virtual Cell Filters in a Microfluidic System for Continuous Isolation and Purification of Circulating Tumour Cells (CTCs) Based on Their Size Characteristics. *Sens Actuators B Chem.* **2017**, *241*, 245−254.
(99) Zhao, Q.; Yuan, D.; Zhang, J.; Li, W. A Review of Secondary Flow in Inertial Microfluidics. *Micromachines (Basel)* **2020**, *11* (5), 461.
(100) Shiriny, A.; Bayareh, M. Inertial Focusing of CTCs in a Novel Spiral Microchannel. *Chem. Eng. Sci.* **2021**, *229*, No. 116102.
(101) Hou, H. W.; Warkiani, M. E.; Khoo, B. L.; Li, Z. R.; Soo, R. A.; Tan, D. S. W.; Lim, W. T.; Han, J.; Bhagat, A. A. S.; Lim, C. T. Isolation and Retrieval of Circulating Tumor Cells Using Centrifugal Forces. *Sci. Rep* **2013**, *3*, 1−8.
(102) Cai, S.; Deng, Y.; Wang, Z.; Zhu, J.; Huang, C.; Du, L.; Wang, C.; Yu, X.; Liu, W.; Yang, C.; Wang, Z.; Wang, L.; Ma, K.; Huang, R.; Zhou, X.; Zou, H.; Zhang, W.; Huang, Y.; Li, Z.; Qin, T.; Xu, T.; Guo, X.; Yu, Z. Development and Clinical Validation of a Microfluidic-Based Platform for CTC Enrichment and Downstream Molecular Analysis. *Front Oncol* **2023**, *13*, 1−18.
(103) Sun, J.; Li, M.; Liu, C.; Zhang, Y.; Liu, D.; Liu, W.; Hu, G.; Jiang, X. Double Spiral Microchannel for Label-Free Tumor Cell Separation and Enrichment. *Lab Chip* **2012**, *12* (20), 3952.
(104) Di Carlo, D.; Irimia, D.; Tompkins, R. G.; Toner, M. Continuous Inertial Focusing, Ordering, and Separation of Particles in Microchannels. *Proc. Natl. Acad. Sci. U. S. A.* **2007**, *104* (48), 18892−18897.
(105) Mansor, M. A.; Takeuchi, M.; Nakajima, M.; Hasegawa, Y.; Ahmad, M. Electrical Impedance Spectroscopy for Detection of Cells in Suspensions Using Microfluidic Device with Integrated. *Applied Sciences* **2017**, *7* (2), 170.
(106) Patel, J. N.; Kaminska, B.; Gray, B. L.; Gates, B. D. PDMS as a Sacrificial Substrate for SU-8-Based Biomedical and Microfluidic

https://doi.org/10.1021/acsomega.4c08606
ACS Omega 2025, 10, 6306−6322

Applications. *Journal of Micromechanics and Microengineering* **2008**, *18* (9), 095028.
(107) Abidin, U.; Daud, N. A. S. M.; Le Brun, V. Replication and Leakage Test of Polydimethylsiloxane (PDMS) Microfluidics Channel. *AIP Conf Proc.* **2019**, *2062*, 020064.
(108) Mansor, M. A.; Ahmad, M. R.; Petrů, M.; Rahimian Koloor, S. S. An Impedance Flow Cytometry with Integrated Dual Microneedle for Electrical Properties Characterization of Single Cell. *Artif Cells Nanomed Biotechnol* **2023**, *51* (1), 371−383.
(109) Tang, W.; Zhu, S.; Jiang, D.; Zhu, L.; Yang, J.; Xiang, N. Channel Innovations for Inertial Microfluidics. *Lab Chip* **2020**, *20* (19), 3485−3502.
(110) Chen, Z.; Zhao, L.; Wei, L.; Huang, Z.; Yin, P.; Huang, X.; Shi, H.; Hu, B.; Tian, J. River Meander-Inspired Cross-Section in 3D-Printed Helical Microchannels for Inertial Focusing and Enrichment. *Sens Actuators B Chem.* **2019**, *301*, No. 127125.
(111) Shi, R. Numerical Simulation of Inertial Microfluidics: A Review. *Engineering Applications of Computational Fluid Mechanics* **2023**, *17* (1), 1.
(112) Zhao, L.; Gao, M.; Niu, Y.; Wang, J.; Shen, S. Flow-Rate and Particle-Size Insensitive Inertial Focusing in Dimension-Confined Ultra-Low Aspect Ratio Spiral Microchannel. *Sens Actuators B Chem.* **2022**, *369* (July), No. 132284.
(113) Nam, J.; Lim, H.; Kim, D.; Jung, H.; Shin, S. Continuous Separation of Microparticles in a Microfluidic Channel via the Elasto-Inertial Effect of Non-Newtonian Fluid. *Lab Chip* **2012**, *12* (7), 1347−1354.
(114) Bhattacharjee, R.; Kumar, R.; Panwala, F. C.; Shakeel, P. M. Design and Analysis of an Optimized Microfluidic Channel for Isolation of Circulating Tumor Cells Using Deterministic Lateral Displacement Technique. *Complex and Intelligent Systems* **2020**, *6* (3), 711−720.
(115) Nan, X.; Zhang, J.; Wang, X.; Kang, T.; Cao, X.; Hao, J.; Jia, Q.; Qin, B.; Mei, S.; Xu, Z. Design of a Low-Frequency Dielectrophoresis-Based Arc Microfluidic Chip for Multigroup Cell Sorting. *Micromachines (Basel)* **2023**, *14* (8), 1561.
(116) Honrado, C.; Bisegna, P.; Swami, N. S.; Caselli, F. Single-Cell Microfluidic Impedance Cytometry: From Raw Signals to Cell Phenotypes Using Data Analytics. *Lab Chip* **2021**, *21* (1), 22−54.
(117) Tran Thi, Y-V.; Hoang, B.-A.; Thanh, H. T.; Nguyen, T.-H.; Ngoc, T. P.; Thu, H. B.; Hoang, N. N.; Bui, T. T.; Duc, T. C.; Do Quang, L. Design and Numerical Study on a Microfluidic System for Circulating Tumor Cells Separation from Whole Blood Using Magnetophoresis and Dielectrophoresis Techniques. *Biochem Eng. J.* **2022**, *186* (June), No. 108551.
(118) Alkhaiyat, A. M.; Badran, M. Numerical Simulation of a Lab-on-Chip for Dielectrophoretic Separation of Circulating Tumor Cells. *Micromachines (Basel)* **2023**, *14* (9), 1769.
(119) Varmazyari, V.; Habibiyan, H.; Ghafoorifard, H.; Ebrahimi, M.; Ghafouri-Fard, S. A Dielectrophoresis-Based Microfluidic System Having Double-Sided Optimized 3D Electrodes for Label-Free Cancer Cell Separation with Preserving Cell Viability. *Sci. Rep* **2022**, *12* (1), 1−14.

https://doi.org/10.1021/acsomega.4c08606
ACS Omega 2025, 10, 6306−6322